

On the Causes of Electrical Conductivity Anomalies in Tectonically Stable Lithosphere

Kate Selway

Received: 30 September 2012 / Accepted: 17 April 2013 / Published online: 16 May 2013
© Springer Science+Business Media Dordrecht 2013

Abstract Magnetotelluric (MT) data can image the electrical resistivity of the entire lithospheric column and are therefore one of the most important data sources for understanding the structure, composition and evolution of the lithosphere. However, interpretations of MT data from stable lithosphere are often ambiguous. Recent results from mineral physics studies show that, from the mid-crust to the base of the lithosphere, temperature and the hydrogen content of nominally anhydrous minerals are the two most important controls on electrical conductivity. Graphite films on mineral grain boundaries also enhance conductivity but are stable only to the uppermost mantle. The thermal profile of most stable lithosphere can be well constrained, so the two important unknowns that can affect the conductivity of a lithospheric section are hydrogen content and graphite films. The presence of both of these factors is controlled by the geological history of the lithosphere. Hydrogen in nominally anhydrous minerals behaves as an incompatible element and is preferentially removed during melting or high-temperature tectonothermal events. Grain-boundary graphite films are only stable to ~ 900 °C so they are also destroyed by high-temperature events. Conversely, tectonic events that enrich the lithosphere in incompatible elements, such as interaction with fluids from a subducting slab or a plume, can introduce both hydrogen and carbon into the lithosphere and therefore increase its electrical conductivity. Case studies of MT results from central Australia and the Slave Craton in Canada suggest that electrical conductivity can act as a proxy for the level of enrichment in incompatible elements of the lithosphere.

Keywords Magnetotellurics · Electrical resistivity · Cratons · Lithosphere · Hydrogen · Graphite

K. Selway
Centre for Tectonics, Resources and Exploration, University of Adelaide, Adelaide, SA 5005, Australia

Present Address:

K. Selway (✉)
Department of Geology and Geophysics, Yale University, 210 Whitney Ave., New Haven, CT 06511,
USA
e-mail: katherine.selway@yale.edu

1 Introduction

Magnetotellurics (MT) is a passive, electromagnetic geophysical method that has sufficient depth penetration to image the electrical resistivity of whole of the lithosphere (Jones and Ferguson 2001; Heinson and Constable 1992; Egbert and Booker 1992; Jones 1999; Muller et al. 2009). It stands with seismic tomography as the only geophysical techniques able to accurately resolve lithospheric-scale features. Therefore, the electrical character of the lithosphere has the potential to be one of its best understood parameters. However, the relationship between electrical resistivity and geological features is often not well understood and this has limited the contribution of MT data to our understanding of the lithosphere. These interpretational difficulties have stemmed largely from insufficient data on the expected resistivities of different mineral systems at lithospheric pressure and temperature conditions and on the possible causes of enhanced conductivity in stable lithosphere. In recent years, numerous experiments in mineral physics have bridged this gap and have provided much of the data necessary to make more geologically meaningful interpretations of MT data. By combining MT data with results from mineral physics experiments and an understanding of the compositional effects of various geological processes, MT can contribute to improving our understanding of lithospheric composition, structures and processes.

MT data measure the electrical resistivity of the Earth by utilizing the fact that time variations in the Earth's magnetic field induce currents in conductive bodies within the Earth. The fluctuations in the Earth's magnetic field are sourced from electrical storms at periods shorter than ~ 1 s and from the interaction between the ionosphere and the solar wind at periods longer than ~ 1 s. Due to the distant origin of the magnetic source fields and the period range of interest, MT fields are considered to be plane waves that are vertically incident on the Earth's surface before traveling in a diffusive manner within the Earth (e.g., Dmitriev and Berdichevsky 1979). The depth of penetration for an MT signal is dependent on the period of the signal and the resistivity of the Earth, such that deepest penetrations will result from a long recording time (typically in the order of several weeks for lithospheric-scale surveys) and a resistive Earth. Electric and magnetic fields are measured in orthogonal directions at the Earth's surface, and the resulting time series are Fourier-transformed into the frequency domain. The ratio of the square of the total magnetic field to the induced electric field at a given period is proportional to the apparent resistivity of the Earth. Therefore, by measuring MT signals at numerous stations along a profile or in a grid and inverting the data, lateral and vertical changes in the electrical resistivity of the Earth can be determined.

There are several potential causes of enhanced conductivity in the lithosphere. Ionic conduction occurs in interconnected saline fluids and can result in low-resistivity zones in porous sedimentary rocks (e.g., Hautot et al. 2000; Hoffmann-Rothe et al. 2001; Tournier and Chouteau 2005; Selway et al. 2012), in regions where water may infiltrate shear zones above the brittle–ductile transition in the mid- to upper crust (Becken and Ritter 2012; Ritter et al. 2005) or where metamorphic fluids are being released from active dehydration reactions (e.g., Wannamaker et al. 2002, 2009; Bertrand et al. 2009). Ionic conduction also occurs in interconnected melts with resulting low-resistivity zones observed beneath areas of active volcanism or tectonism (ten Grotenhuis et al. 2005; Schilling et al. 1997; Brasse et al. 2002; Hill et al. 2009). The focus of this review is the interpretation of MT data in tectonically stable, cratonic lithosphere. In such regions, by definition, active tectonism is not occurring and low-resistivity zones caused by melts or metamorphic fluids would not be expected. Saline fluids may cause low-resistivity zones in the upper crust, but free,

interconnected fluid would not be expected to exist at greater depths within the lithosphere. These conduction mechanisms will therefore not be a focus of this discussion.

Sulfide minerals have low resistivity, and interconnected sulfides have been interpreted to be the cause of some low-resistivity features in cratonic environments (Chouteau et al. 1997; Livelybrooks et al. 1996; Jones et al. 2005a). While interconnected sulfides are of importance in selected settings, they are not expected to be a common cause of enhanced conductivity in the lithosphere. Sulfides are not volumetrically abundant (sulfur is only ~0.7 wt% of a bulk Earth composition (Allegre et al. 1995)) and are generally unstable at depths greater than the uppermost mantle (e.g., Sack and Ebel 2006) so anomalies due to such minerals will generally be discrete, small-scale features. In a recent study, Watson et al. (2010) found that a small amount (1.4 wt%) of FeS powder added to finely ground (~45 ηm) olivine formed films on the olivine grain boundaries that enhanced conductivity by more than an order of magnitude. Since it does not currently appear common for natural samples to exhibit such films and the measured grain sizes are much smaller than average lithosphere, which would enhance grain-boundary conduction (see discussion in Sect. 2.1), these films will also not be a focus of this review. However, given the stark increase in conductivity measured by Watson et al. (2010), such films would produce an observable response if further research can predict circumstances in which they might exist.

Since fluids, melt and interconnected sulfides are unlikely to account for significant conductivity anomalies in the stable lithosphere, only two primary candidates remain to explain such observations: conduction through grain-boundary graphite films and semi-conduction through diffusing particles in silicate minerals. In order to produce geologically meaningful interpretations of MT data, it is therefore necessary to understand the geological factors that lead to enhancement of or reduction in these two components. In this review, conduction through both silicate semi-conduction and grain-boundary graphite films is summarized and it is argued that each of these conduction mechanisms will be most abundant in lithosphere that is enriched in incompatible elements, which are elements that preferentially partition into melt during partial melting. This summary is followed by a discussion about the thermal and compositional structure of cratonic lithosphere in terms of the factors that will lead to enrichment or depletion in incompatible elements. It is shown that lithosphere that has experienced multiple generations of melting events will be depleted but that such lithosphere may be re-fertilized by interaction with melts from a subducting slab or a mantle plume. With this in mind, MT results from the Archean to Paleoproterozoic Gawler Craton and Mesoproterozoic to Neoproterozoic Musgrave Province in Australia and from the Archean Slave Craton in Canada are reviewed. The analysis shows that those parts of the lithosphere that have been re-fertilized by subduction or plume events have higher conductivities than would be expected for dry, crystalline lithosphere with no conducting phase, whereas those that have undergone high-temperature metamorphic and melting events have high resistivities that suggest that no enhanced conductivity is present. It is suggested that, for stable lithosphere, MT data be interpreted with a consideration of the expected enrichment state of the lithosphere (e.g., Wannamaker 2005; Yang et al. 2011).

2 Electrical Conduction Mechanisms in Stable Lithosphere

The first step in seeking to make meaningful interpretations of MT data must be to know the expected resistivities of common mineral assemblages at lithospheric pressure and

temperature conditions by reviewing findings from relevant mineral physics experiments. It is only through comparing such data with MT models that it is possible to know whether additional phases need to be invoked to explain the modelled resistivity.

2.1 Diffusion in Semi-conductors

While silicate minerals behave as resistors at surface pressures and temperatures, at depths as shallow as the lower crust they begin to behave as semi-conductors. The charge carriers for semi-conduction are diffusing particles (see Chakraborty (2008) for a review of diffusion in silicates) and conductivity σ obeys the Nernst–Einstein equation:

$$\sigma = Nze\mu$$

where N is the number of electric charge carriers per unit volume, z is the charge number, e is the charge of an electron, and μ is the mobility. Conduction by diffusing species is defined by the Arrhenius relation:

$$\sigma = \sigma_0 \cdot \exp\left(\frac{-\Delta H}{RT}\right)$$

where σ_0 is the pre-exponential factor, ΔH is the activation enthalpy, R is the gas constant, and T is the absolute temperature.

The physical manifestation of these relationships is that composition and temperature are the two most important factors controlling the conductivity of silicates. Composition is important because it determines which species are available to diffuse. Experiments on nominally anhydrous minerals which dominate the lithosphere such as olivine (Poe et al. 2010; Wang et al. 2006, 2012; Yoshino et al. 2006, 2009), garnet (Dai et al. 2012; Mookherjee and Karato 2010; Yoshino et al. 2008), orthopyroxene (Dai and Karato 2009a; Yang et al. 2012), clinopyroxene (Yang et al. 2011) and plagioclase (Yang et al. 2012) have concluded that hydrogen content is the most important compositional parameter affecting conductivity at lithospheric temperatures and pressures (Karato 1990, 2006; Yoshino 2010). Other compositional factors such as mineralogy (e.g., Dai and Karato 2009b; Yang et al. 2012) and magnesium number ($Mg\# = Mg/(Mg + Fe)$) (Dai et al. 2012; Yoshino et al. 2009) have important but lesser effects on conductivity (Fig. 1). Given the importance of hydrogen concentration to conductivity, experiments with controlled and measured water contents will be focused on in the following discussion. Temperature must be sufficiently high to overcome the activation enthalpy of diffusion, and an increasing temperature will increase the efficiency of diffusion. In many systems, the most efficient diffusion regime will change with increasing temperature as different particles gain sufficient energy to overcome their activation enthalpy (Chakraborty 2008; Yoshino 2010).

Olivine ($(Mg,Fe)_2SiO_4$) is the dominant mineral in the upper mantle and its conductivity has been extensively studied in mineral physics experiments. Although some findings differ with different experimental methods between groups (Yoshino 2010; Yang et al. 2012; Karato and Dai 2009), the experimental data agree that, at temperatures representative of the lithospheric mantle, conduction in hydrous olivine is dominated by hydrogen diffusion (Yoshino et al. 2009; Wang et al. 2006, 2012; Poe et al. 2010; Karato 2006). Hydrogen sits in the mineral lattice of hydrated olivine (or other nominally anhydrous minerals) as a point defect (e.g., Karato 2006; Kohlstedt and Mackwell 1998) and therefore requires a lower activation enthalpy to diffuse than more stable species. At higher

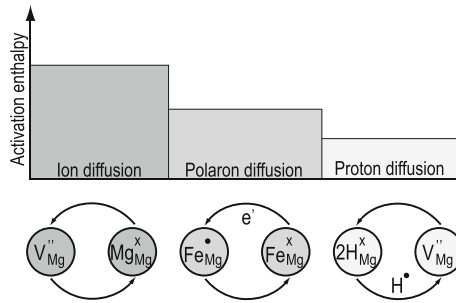


Fig. 1 Schematic illustration of the main diffusion mechanisms in (Fe, Mg) silicates using the Kröger-Vink notation X_Y^Z where species X occupies site Y with charge Z , V is a vacancy, $'$ is a negative charge, x is neutral charge and $^{\bullet}$ is a positive charge. Ionic diffusion involves the diffusion of iron or magnesium ions with a site vacancy and has a high activation enthalpy. Polaron diffusion involves the diffusion of an electron between ferrous and ferric iron and has a moderate activation enthalpy. Proton diffusion involves the diffusion of hydrogen ions (diffusion with a vacancy is illustrated, but diffusion may involve other species) and has a low activation enthalpy

temperatures representative of the upper mantle but dependent on the specific composition of interest (Yoshino et al. 2009, 2012), the system has sufficient energy to overcome the activation enthalpy for diffusion of electron holes between ferric (Fe^{3+}) and ferrous (Fe^{2+}) ions (Schock et al. 1989; Kohlstedt and Mackwell 1998; Chakraborty 2008) in a process called small polaron conduction. In this regime, the major element chemistry of olivine is important and an increase in iron concentration (or decrease in magnesium number) will increase conductivity as it results in a greater concentration of diffusing particles (Yoshino et al. 2009, 2012). In addition, a decrease in the activation enthalpy has been measured with increasing iron content, interpreted to be due to a decreasing average distance between Fe^{2+} and Fe^{3+} ions (Yoshino 2010). In the polaron conduction regime, the effects of polaron conduction and hydrogen conduction will be cumulative such that, at these temperatures, hydrous olivine will still be more conductive than anhydrous olivine (Poe et al. 2010; Wang et al. 2006; Yoshino et al. 2009). At temperatures that are higher still and approach the melting temperature of olivine, diffusion between iron and magnesium ions and lattice vacancy sites begins to occur (Schock et al. 1989) (Figs. 1, 2).

Semi-conduction in other nominally anhydrous mantle silicate minerals follows the same pattern as in olivine. Experimental results on orthopyroxene show higher conductivities and lower activation enthalpies for hydrous samples than dry samples (Dai and Karato 2009a; Xu and Shankland 1999). Activation energies are similar to those measured in olivine, suggesting that the conduction mechanisms are the same, but the absolute conductivities of both dry and hydrous orthopyroxene are higher than those of olivine (Dai and Karato 2009a). Likewise, hydrous garnet has a higher conductivity and lower activation enthalpy than dry garnet, but the conductivity of garnet is higher than that of olivine and orthopyroxene at the same temperature, pressure and hydration conditions (Dai and Karato 2009a, b). Measurements taken at temperatures corresponding to the polaron diffusion regime demonstrate that garnets with higher iron contents have higher conductivities at given pressure and temperature conditions (Yoshino et al. 2008; Dai et al. 2012). Figure 3 shows a comparison of experimental ranges from different laboratories of resistivities of dry and hydrous olivine, pyroxene and garnet, adapted from a compilation by Fullea et al. (2011).

Fig. 2 Schematic plot of the change in conduction mechanism with temperature. With increasing temperature, the most efficient conduction mechanism changes from proton conduction to small polaron conduction to ionic conduction. Proton conduction is dependent on hydrogen concentration, and small polaron conduction is dependent on iron concentration. The specific temperature at which the dominant conduction mechanism changes is compositionally dependent

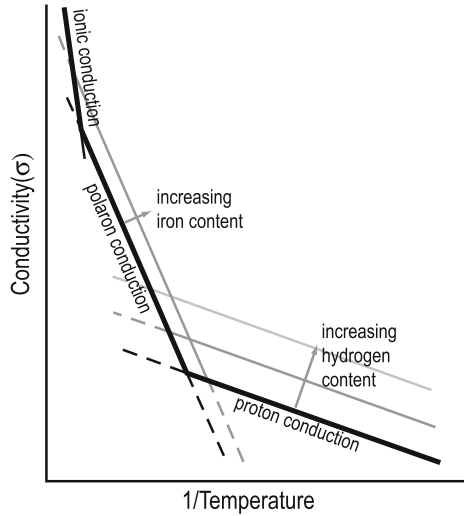
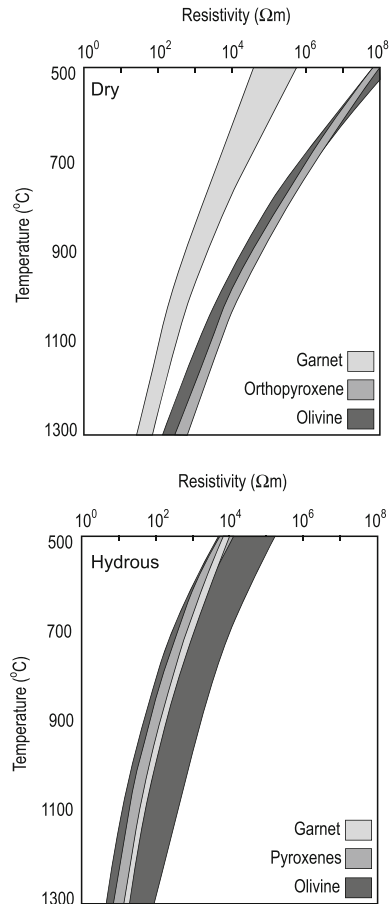


Fig. 3 Resistivity versus temperature data for selected experimental results of mantle minerals described in the text and adapted from the compilation of Fullea et al. (2011) for a temperature range representing the lithospheric mantle. The upper plot shows results for the resistivity of dry olivine from Yoshino et al. (2009) and Wang et al. (2006), dry orthopyroxene from Dai and Karato (2009a), and dry garnet from Dai and Karato (2009b) and Yoshino et al. (2008). The lower plot shows results for the resistivity of hydrous olivine (400 wt ppm H_2O) from Wang et al. (2006), Yoshino et al. (2009) and Poe et al. (2010), hydrous orthopyroxene (200 wt ppm H_2O) and hydrous clinopyroxene (400 wt ppm H_2O) from Dai and Karato (2009a), and hydrous garnet (20 wt ppm H_2O) from Dai and Karato (2009b)



Measurements of the conductivities of crustal nominally anhydrous minerals show similar trends to those seen in the mantle minerals described above. Yang et al. (2012, 2011) measured orthopyroxene, clinopyroxene and plagioclase, which are the main constituents of stable lower crust, at both dry and hydrous conditions. As for mantle minerals, dry orthopyroxene, clinopyroxene and plagioclase have higher activation enthalpies and lower conductivities than hydrous minerals and there is evidence that higher iron contents in the pyroxenes and sodium content in the plagioclase decrease the activation enthalpy of the dry minerals (Yang et al. 2011, 2012). Plagioclase has the lowest conductivity of the three minerals in both the dry and hydrous cases, while the conductivity of orthopyroxene is slightly higher than that of clinopyroxene at the same conditions of hydration (Yang et al. 2012). However, in nature, water partitions preferentially into clinopyroxene so it is likely that clinopyroxene would dominate the conductivity of a hydrous lower crust if interconnected (Yang et al. 2012).

Oxygen fugacity also affects electrical conductivity at a given composition and temperature (e.g., Dai et al. 2012; Karato 2011; Dai and Karato 2009c). In the small polaron diffusion regime, an increase in oxygen fugacity will increase the proportion of ferric (Fe^{3+}) ions and will therefore increase conductivity. In the hydrogen diffusion regime, an increase in oxygen fugacity will have the opposite effect, decreasing the number of hydrogen point defects and decreasing conductivity. Experimental data for garnet at temperature and pressure conditions typical of the upper mantle show that the effect of oxygen fugacity is less than that of temperature and hydration but is still significant, with conductivities differing by approximately half an order of magnitude between the highest ($\text{Fe}_2\text{O}_3 + \text{Fe}_3\text{O}_4$) and lowest ($\text{Mo} + \text{MoO}_2$) oxygen buffers (Dai et al. 2012). As depth increases through the continental lithospheric column, oxygen fugacity is expected to systematically decrease by three to four orders of magnitude due to increasing pressure and changing mineral stability fields (Frost et al. 2008; Wood et al. 1990). Therefore, dry conductivity will systematically increase with depth, and wet conductivity will systematically decrease. While pressure affects the conductivity through changing oxygen fugacity, its direct impact on conductivity within the stability field of the mineral being measured is minimal (e.g., Xu et al. 2000; Yang et al. 2011; Yoshino 2010). Studies show that conductivity may be anisotropic for some lithospheric minerals. Although the strength of conductivity anisotropy is debated, it appears to increase with water content and to be strongly temperature-dependent (Poe et al. 2010; Yoshino et al. 2006; Du Frane and Tyburczy 2012; Du Frane et al. 2005; Wang et al. 2006). The reader is directed to the review by Pommier (2013) in this volume for a more thorough discussion.

Hydrogen diffusion, small polaron diffusion and ion diffusion are all volume diffusion processes, that is, the particles diffuse through the interior of the crystal lattice. However, diffusion of point defects can also occur along grain boundaries (Chakraborty 2008). Studies directly investigating the influence of grain size on conductivity suggest that grain-boundary diffusion becomes important only at very small grain sizes (Fig. 4). For instance, Demouchy (2010a) showed that, depending on diffusion mechanism and crystallographic axis, diffusion is independent of grain size for grain sizes greater than a minimum of 0.01 mm and a maximum of 1 mm. ten Grotenhuis et al. (2004) measured an increase in conductivity with decreasing grain size for synthetic forsterite but only for a narrow range of very small grain sizes (1.1 ± 0.4 to $4.7 \pm 2.4 \mu\text{m}$), for which hydrogen contents were not measured. In contrast, Yang et al. (2011) and Yang and Heidelbach, (2012) observed no difference in conductivity between polycrystalline samples of clinopyroxene with grain sizes 5–250 μm and larger single crystals of approximately 1 mm. The majority of mineral physics experiments carried out on polycrystalline aggregates described in the preceding

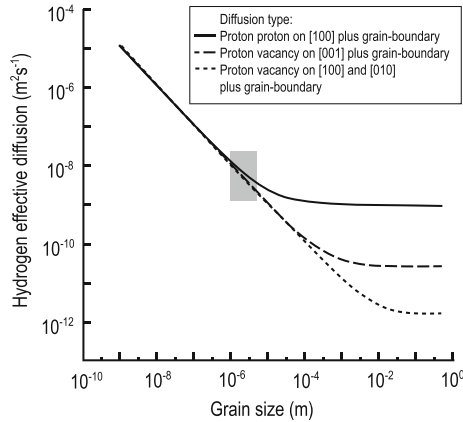


Fig. 4 Experimental results showing the grain-size dependence of grain-boundary diffusion in olivine at 1,200 °C and 300 MPa, adapted from Demouchy (2010a). The steep gradient at small grain sizes indicates faster diffusion along grain-boundaries, whereas at larger grain sizes, the flat gradient shows that grain-boundary diffusion is less efficient than lattice diffusion and that grain size will not affect resistivity. The grey box indicates the range of grain sizes included in the experiments of ten Grotenhuis et al. (2004). At grain sizes typical of the upper mantle (>1 mm), the effect of grain-boundary diffusion will be minimal

section observed only volume diffusion, even at grain sizes of 1 μm , suggesting that grain-boundary diffusion did not contribute significantly to conduction (e.g., Dai and Karato 2009c; Wang et al. 2006; Yoshino et al. 2009). Therefore, while more experimental results are needed, it is reasonable to expect that increases in conductivity with decreasing grain size may only be apparent for grain sizes smaller than 10–100 μm , if at all. Given that typical grain sizes in the lithospheric mantle are on the order of 1 mm and smaller grain sizes ($\sim \leq 10 \mu\text{m}$) only expected in specific settings such as shear zones, small grain size is not likely to be the cause of large conductive anomalies.

Combined analysis of seismic and MT data can be very powerful in discriminating between the different causes of enhanced conduction by semi-diffusion. Seismic velocities are strongly dependent on major element chemistry and will be substantially reduced by an increasing Fe content, but are only slightly reduced by the addition of substantial amounts of hydrogen. In contrast, seismic attenuation is strongly dependent on hydrogen content, has a modest dependence on grain size and shows little variation with major element chemistry (Karato 2006 and references therein). Joint analysis of appropriate datasets therefore has potential to be a powerful tool for constraining lithospheric composition (e.g., Jones et al. 2013).

2.2 Grain-Boundary Graphite Films

Graphite films with thicknesses from as small as several nm up to several hundred nm have been observed on the grain boundaries of minerals from many mid- to lower crustal samples (Frost et al. 1989; Mareschal et al. 1992; Mathez et al. 1995). Experimental results show that the presence of interconnected graphite films on grain boundaries can increase the conductivity of a sample by several orders of magnitude (e.g., Glover 1996) and have provided a feasible interpretation of low-resistivity zones in the graphite stability field within the crust and upper mantle (e.g., Jones et al. 2003; Santos et al. 2002; Mareschal et al. 1995) that in some cases has been proven through petrological identification of

graphite in the conductor and petrophysical analysis of rock samples (Jödicke et al. 2004; Pous et al. 2004). It is necessary to understand the habit of carbon in order to predict its conductivity since individual flakes of graphite (e.g., Jödicke et al. 2004), unconnected grain-boundary films (e.g., Katsube and Mareschal 1993) or carbon trapped in fluid inclusions will not enhance conductivity. More detail on the conditions in which graphite would be expected to exist as grain-boundary films is given in Sect. 3.2.

3 Expected Resistivity Structure of Stable Continental Lithosphere

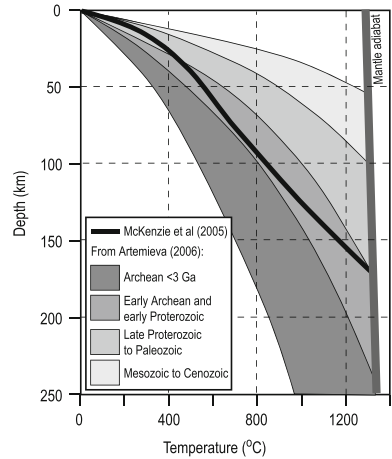
Cratons are stable pieces of lithosphere that have remained largely undeformed since the Proterozoic. Cratonic sub-continental lithospheric mantle (SCLM) is expected to be dominantly Archean in age since Proterozoic crust exposed at the surface of cratons appears to be generally underlain by Archean SCLM (Griffin et al. 2009). Given the age and stability of cratonic lithosphere, several generalizations can be made about its structure, composition and temperature profile. Since the factors that control lithospheric conductivity are temperature, hydrogen content and graphite films, this analysis will focus on the thermal structure of the lithosphere, the mechanisms by which hydrogen is incorporated into nominally anhydrous minerals and the expected settings in which hydrogen and graphite films would be present.

3.1 Thermal Structure of the Lithosphere

Compilations of average surface heat flow from Archean and Proterozoic regions show that heat flow statistically decreases with increasing age of the lithosphere, from an average of 41 ± 11 mW/m² in Archean regions to 55 ± 17 mW/m² in Proterozoic regions not associated with Archean lithosphere (Nyblade and Pollack 1993). The thermal structure of the lithosphere associated with these heat flows is dependent on the partitioning of radioactive elements (and therefore heat production) between the crust and the mantle and on the thickness of the lithosphere (Nyblade and Pollack 1993; Rudnick et al. 1998; Jaupart and Mareschal 2007). Combined analysis of seismological data, heat flow data, pressure and temperature estimates from xenoliths and compositional constraints from xenoliths have allowed well-constrained models of average lithospheric thermal structure to be produced (Fig. 5) (McKenzie et al. 2005; Rudnick et al. 1998; Artemieva and Mooney 2001; Artemieva 2006) with uncertainties as little as 100–200 °C (Artemieva and Mooney 2001). However, individual regions may depart from these averages. For instance, stable Proterozoic lithosphere in central and southern Australia has surface heat flows that exceed 100 mW/m² due to high concentrations of radioactive elements. In contrast, the Tanzanian Craton has surface heat flow values as low as 13 mW/m² (Nyblade et al. 1990), but the temperature at the base of the lithosphere is elevated by ~ 150 °C due to the present-day thermal impact of a plume (Lee and Rudnick 1999). Since temperature exerts a strong influence on conductivity (as described in Sect. 2.1), it is important to consider the specific thermal regime of the region of interest in interpreting MT data. For instance, a Phanerozoic setting or a region of high heat flow would be expected to exhibit higher conductivities than an Archean or other low heat flow setting for a given depth even if all other compositional factors were identical.

The thermal history of the lithosphere can also control its composition and therefore also its conductivity. For instance, at high temperatures, grain-boundary graphite films become unstable and minerals are likely to dehydrate (see Sect. 3.3) which will increase

Fig. 5 Solid line shows the thermal gradient of stable continental lithosphere calculated by McKenzie et al. (2005). Greyscale regions show the average thermal gradients of lithosphere of different ages calculated by Artemieva (2006) on the basis of surface heat flow and xenolith data



lithospheric resistivity even after the thermal structure has stabilized. Mantle temperatures would have been approximately 150 °C higher toward the end of the Archean (Michaut et al. 2009), so depths of temperature-controlled reactions would have been shallower. Tectonic events such as collision, accretion, delamination and rifting will also result in increased lithospheric temperatures. Specific thermal histories can be determined through petrological analysis of metamorphic rocks; for instance, ultra-high-temperature metamorphic mineral assemblages representing lower crustal temperatures ≥ 900 °C have been interpreted to be formed in accretionary back-arc basins, collisional systems and through contact metamorphism (Kelsey 2008). Determination of the thermal history of the lithosphere may allow the causes of an observed resistivity structure to be constrained.

3.2 Distribution of Grain-Boundary Graphite Films

For graphite to cause significant conductivity anomalies, two main conditions must be met: first, the lithosphere must contain sufficient carbon to form the requisite thickness of graphite, and second, the graphite must be interconnected, which will generally be in the form of grain-boundary films. Estimates of mid-ocean ridge basalt (MORB) carbon content vary from 10 to 30 ppm, while estimates of enriched mantle vary from 50 to 500 ppm (Dasgupta and Hirschmann 2010). Since grain-boundary films as thin as several nm will enhance conductivity, geologically reasonable carbon concentrations of the order of 100 ppm can produce a conductivity anomaly if the graphite is interconnected (Duba and Shankland 1982). Xenolith samples display a range of carbon contents, suggesting that the distribution of carbon in the SCLM is not uniform. Interaction with kimberlitic or subduction-related melts, which are rich in carbon (Sleep 2009; Plank and Langmuir 1998), will increase the carbon content of the SCLM, as discussed in greater detail in Sect. 3.5. The different sources of carbon in the mantle may be distinguished by $\delta^{13}\text{C}$ isotopes whereby “heavy” $\delta^{13}\text{C}$ signatures (~ -5 ‰) have been interpreted to represent a mantle source and “light” $\delta^{13}\text{C}$ signatures (~ -25 ‰) have been interpreted to represent a subducted organic matter source (e.g., Sano and Marty 1995; Pearson et al. 1994; Tappert et al. 2005). However, some caution should be applied to these interpretations as Deines (2002) argues that the different $\delta^{13}\text{C}$ signatures may simply represent different mantle C reservoirs.

Carbon in the lithosphere can exist as diamonds, fluid inclusions, CH₄, carbonate minerals, CO₂-bearing melt or fluids, individual graphite flakes and as grain-boundary graphite films. In stable lithosphere in which we assume no melt is present, it is only the latter form that will create a significant conductor so it is important to determine the conditions under which grain-boundary graphite films will form. Diamonds and graphite both require reducing conditions (approximately 1.5–2.5 log units below the fayalite-magnetite-quartz (FMQ) oxygen fugacity buffer) for stability (Stagno and Frost 2010). At more oxidizing conditions, diamonds and graphite become unstable, converting to carbonate minerals at temperatures below the solidus and to a carbon-rich melt at temperatures above the solidus. Graphite is stable at pressures and temperatures less than ~5 GPa and 1,100 °C, corresponding to a depth of approximately 150 km in a standard cratonic geotherm, while diamond is stable at greater depths (Pearson et al. 1994). However, even within the graphite stability field, grain-boundary graphite films appear to have a limited stability range. Analysis of xenoliths suggests that grain-boundary graphite films are only stable to temperatures of approximately 600–900 °C (Mathez 1987; Mathez et al. 1984; Pineau and Mathez 1990). Likewise, in conductivity measurements, Yoshino and Noritake (2011) found that the conductivity of grain-boundary graphite films on synthetic quartz crystals decreased rapidly at temperatures >1,000 °C as the graphite films became unstable. At very shallow depths, low pressures appear to break the connection pathways between the graphite films such that they no longer form a conductor (e.g., Katsube and Mareschal 1993; Duba et al. 1988, 1994). Grain-boundary graphite films observed on xenoliths have been interpreted to have formed during quenching of the sample, when carbon from volcanic gases was deposited on fresh mineral surfaces (Mathez 1987), which suggests that they are related to low-temperature processes operating in the uppermost mantle or the crust. Kimberlite melts are particularly rich in carbon and are likely to degas CO₂ in the uppermost mantle (Pearson et al. 1994; Sleep 2009; Hunter and McKenzie 1989; Wyllie 1980). The characteristic interstitial angle of the degassed CO₂ is sufficiently low that it can move along grain boundaries (Hunter and McKenzie 1989). In sufficiently reducing conditions, this CO₂ will be converted to graphite and this could be an important source for grain-boundary graphite films.

3.3 Hydrogen Content in Nominally Anhydrous Minerals (NAMs)

Measured hydrogen concentrations in mantle xenoliths generally fall in the ranges 0–0.02 wt% for olivine and garnet (equivalent to 0–200 wt ppm) and 0.01–0.02 wt% for pyroxenes (equivalent to 100–200 wt ppm) (Bell and Rossman 1992). However, it is not necessarily valid to rely on xenolith data to determine the average water content of the upper mantle since xenoliths may lose or gain hydrogen during exhumation (e.g., Ingrin and Skogby 2000) and tend to be sourced from non-representative regions of the lithosphere (Griffin et al. 2009). Experimental studies on dissolution of hydrogen in NAMs show that the hydrogen content is related to the number of appropriate point defects in the mineral lattice combined with the availability of hydrogen ions that can act as a charge compensator in the vacancy (e.g., Karato 2006). The maximum amount of hydrogen that can be incorporated into mantle minerals will increase with increasing pressure and with decreasing oxygen fugacity (Ingrin and Skogby 2000) but at typical upper mantle conditions will be in the order of 0.01 wt% for olivine and garnet and 0.1 wt% for pyroxenes (Ingrin and Skogby 2000; Kohlstedt et al. 1996; Bell et al. 2003; Lu and Keppeler 1997; Mierdel et al. 2007; Kovács et al. 2012).

Hydrogen behaves as an incompatible element in the mantle, meaning that during melting or devolatilization, it will preferentially partition into the melt rather than remain in the solid mineral phase. Michael (1988) analyzed MORB glass samples and found that the samples that were enriched in incompatible elements were also enriched in H₂O. H has approximately the same incompatibility as Ce, and the measured H partition coefficient between olivine and melt is 0.0017 ± 0.0005 , between clinopyroxene and melt is 0.023 ± 0.005 and between orthopyroxene and melt is 0.019 ± 0.004 (Aubaud et al. 2004). In the solid phase, water will partition preferentially into orthopyroxene and clinopyroxene rather than into olivine, whereas most other incompatible elements will partition into clinopyroxene and garnet over orthopyroxene and olivine (Bell and Rossman 1992). Therefore, it is reasonable to expect that hydrogen proportions will broadly follow incompatible element proportions and that “enriched” portions of the lithosphere will have high hydrogen concentrations while “depleted” portions will contain little to no hydrogen. Although lithospheric hydrogen content is difficult to constrain from xenoliths and is not a routine measurement, the level of enrichment or depletion in incompatible elements in xenoliths is a common analysis and their distribution with regard to different geological systems is well understood. By recognizing that regions enriched in other incompatible elements are also likely to be enriched in hydrogen, it is possible to predict the regions in which we would expect high conductivity due to hydrogen.

3.4 Compositional Structure of the Lithosphere

Compositionally, the volumetrically most abundant mineral in the SCLM is olivine, followed by orthopyroxene, clinopyroxene and garnet. Average trends show that mantle composition becomes increasingly depleted in incompatible elements (such as Fe, Al, Ca and radioactive elements) with increasing age (e.g., Djomani et al. 2001) as these volatile elements are preferentially partitioned into melt during melting events (Hofmann 1988; Workman and Hart 2005). Careful analysis by Griffin et al. (2009) to remove bias inherent in determining compositions from xenolith data showed that highly depleted Archean SCLM would have a magnesium number of 93.1. In contrast, the magnesium number of models for mantle that has undergone no depletion events (the primitive upper mantle) is approximately 89.3 (McDonough and Sun 1995) (Fig. 6). Changes in iron content of this magnitude will produce such small changes in conductivity that they will not affect MT results (e.g., Yoshino et al. 2008). In comparisons of xenolith samples made by Kame-netsky et al. (2001), the median of the proportion of forsterite (the magnesium end-member of olivine) in depleted MORB was 89.5, whereas the median value for enriched, plume-derived ocean island basalt was 83.5. This difference is also unlikely to produce a detectable conductivity signature. The difference was more pronounced in spinels (median magnesium number of 71 for MORB and 51 for ocean island basalts) so, if such phases are sufficiently voluminous to be interconnected, a small signal may be detectable. However, other compositional changes are expected to be more important. The models of Griffin et al. (2009) and McDonough and Sun (1995) predict that at 100-km depth, the proportions of olivine/orthopyroxene/clinopyroxene/garnet are 87.8/11.2/0.2/0.9 for depleted Archean SCLM and 55.1/17.9/10.0/17 for primitive mantle that is not depleted in incompatible elements. At 200-km depth, the trend is similar with compositional proportions of 87.8/10.7/0.3/1.2 for depleted Archean SCLM and 55.6/19.6/9.6/15.2 for the primitive mantle (Fig. 6). Undepleted mantle therefore has much higher proportions of pyroxenes and garnet compared to olivine than depleted mantle. Under dry conditions, garnet is approximately an order of magnitude more conductive than olivine at mantle temperatures and the

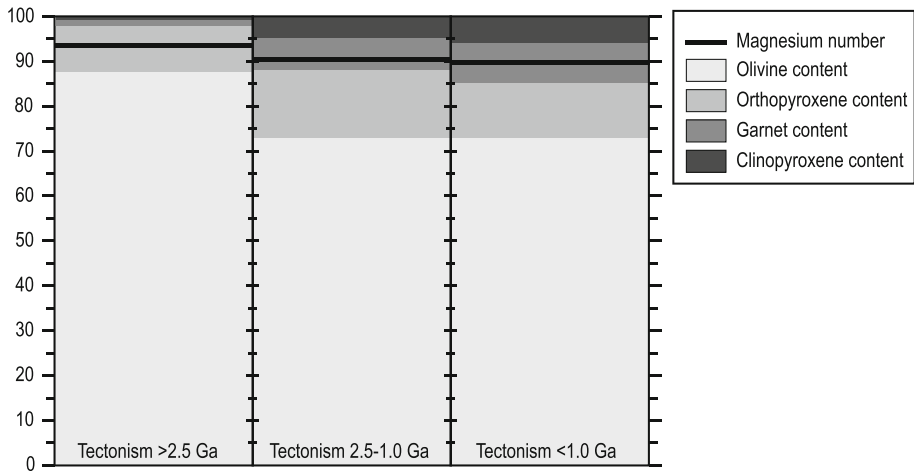


Fig. 6 Average composition at 100 km depth of three types of lithosphere as compiled by Griffin et al. (2009): lithosphere that has experienced no tectonism since 2.5 Ga, lithosphere that has experienced tectonism between 2.5 and 1.0 Ga and lithosphere that has experienced tectonism later than 1.0 Ga. The heavy black line is the magnesium number ($Mg/(Mg + Fe)$), and the solid shaded areas are the proportions of olivine, orthopyroxene, garnet and clinopyroxene

conductivity of orthopyroxene is intermediate between garnet and olivine (under hydrous conditions the difference is reduced) (Dai and Karato 2009a, b). Therefore, it is possible that, given a sufficient, interconnected volume fraction, the increased garnet and pyroxene proportion in primitive mantle may be detectable by MT.

The resistivity of stable lower crust has been imaged in MT surveys to vary greatly from <10 to $>10,000 \Omega m$ worldwide (Jones 1992; Korja and Hjelt 1993; Haak and Hutton 1986; Selway et al. 2011; Jones et al. 2005b). The observation of a lower crustal conductor in many regions has led to significant debate over its possible causes over the last three decades (e.g., Haak and Hutton 1986; Jones 1992; Yardley and Valley 1997; Wannamaker 2000; Yang 2011). Continental crust displays more lithological variation and less clear patterns of secular evolution than the mantle, but some generalizations can still be made about its average expected composition (Taylor and McLennan 1995). In general, since the crust is formed in a fundamental sense by melting of the mantle, it is more enriched in incompatible elements than the mantle and its composition will be determined by the composition of the mantle from which it was extracted (Hofmann 1988). Crustal thickness is dependent on age and tectonic setting, and for cratons, it averages at approximately 40 km, with its base defined as the Moho (Christensen and Mooney 1995). The lower crust (defined as depths greater than 20–25 km) is generally in the granulite facies, a metamorphic regime defined by having reached temperatures greater than approximately 650 °C and pressures greater than 600 MPa, in which amphiboles dehydrate to pyroxenes. Its average composition is mafic with the dominant minerals being orthopyroxene, plagioclase and clinopyroxene (Christensen and Mooney 1995; Rudnick and Fountain 1995). The middle crust (from between 10–15 and 20–25 km depth) is generally considered to be in the amphibolite facies (metamorphism at 450–700 °C and >300 MPa), in which amphiboles are stable, and plagioclase, quartz and amphibole are the dominant mineral species present (Rudnick and Fountain 1995; Christensen and Mooney 1995). In comparison with the mantle, the magnesium number of the crust can vary significantly, for

example varying between approximately 45 and 62 for the samples compiled by Rudnick and Fountain (1995), and may be sufficient to be observed in MT measurements. Yang (2011) has argued that that lower crustal conductors up to $\sim 100 \Omega\text{m}$ can be explained by semi-diffusion in common crustal minerals (Yang and Heidelberg 2012; Yang et al. 2011, 2012) due to their high iron contents and some high measured water contents ($>0.1 \text{ wt}\%$). However, in this analysis, Yang (2011) relied on a lower crustal temperature estimate of 700–1,000 °C, which is much higher than that expected for stable, Precambrian crust (Fig. 5). At a more reasonable lower crustal temperature of 500 °C, laboratory data at even the highest calculated water contents (0.0375 wt% for clinopyroxene, 0.0285 wt% for orthopyroxene and 0.089 wt% for plagioclase) only predict resistivities of between 10^3 and $10^4 \Omega\text{m}$ and are therefore unable to explain lower resistivities sometimes observed in the lower crust.

Alternative interpretations have been in two forms. Early explanations relied on laboratory data that showed that typical lower crustal mineralogies saturated by free saline fluids could reproduce observed high conductivities (Glover and Vine 1994; Hyndman and Hyndman 1968). In stable tectonic settings, free fluid will only exist in the brittle regime and will not extend into the ductile regime where significant pore spaces do not exist (e.g., Kohlstedt et al. 1995; Connolly and Podladchikov 2004). Although the brittle/ductile transition is generally in the mid-crust, in regions with low geotherms, the brittle regime may extend into the lower crust (e.g., Bürgmann and Dresen 2008). However, Yardley and Valley (1997) showed that even if fluids can reach stable lower crust, they will react with wall rocks and be consumed. The stable lower crust is therefore a “sink” for fluids, and no significant volumes of fluid will survive there. Most other interpretations for strong crustal conductors have relied on grain-boundary graphite films, which will be at appropriate pressures to be interconnected throughout much of the crust and, given sufficiently reducing conditions, will be stable. In many cases, this interpretation has been strengthened by a tectonic association with a former suture zone, which is likely to have contained large quantities of carbon-rich sediment, or by a correlation with an outcropping graphite-rich horizon (e.g., Boerner et al. 1996; Jödicke et al. 2004; Hjelt and Korja 1993; Banks et al. 1996; Ogawa et al. 1996). In reality, due to the very heterogeneous nature of the crust, the causes for lower crustal conductivity are likely to differ in different locations (Wannamaker 2000). In some cases, there can be little doubt that the conductors are caused by graphite. In regions of only moderately high conductivity, elevated temperature or very high iron or water contents could produce the conductors. Interconnected sulfides create at least some important crustal conductors (Jones et al. 2005a), and further research on sulfide films (Watson et al. 2010) may cement these as another candidate. As for the rest of the lithosphere, the specific thermal and compositional structure and thermotectonic history of each region of interest should be carefully considered in order to include or exclude possible interpretations.

The upper crust is also highly heterogeneous, and there are many potential causes of upper crustal conductivity anomalies. Conductors caused by graphite or sulfides in the lower crust would be expected to continue to the upper crust so long as the connection pathways do not become broken. In addition, because the upper crust is in the brittle regime and temperatures will generally be too low for metamorphic reactions to consume fluid, free fluids can exist in available pore spaces. Saline fluids are the likely cause of low resistivities observed in many sedimentary basins and aquifers (e.g., Meqbel and Ritter 2013; Selway et al. 2012) and in upper crustal shear zones (Becken and Ritter 2012). Sedimentary basins may also contain layers of shale that are rich in organic matter that will also produce a conductive response (e.g., Branch et al. 2007).

3.5 Compositionally Modified Lithospheric Mantle

While Sect. 3.4 summarized the expected composition of average lithospheric mantle, it is important to note that this composition can be modified by tectonothermal events. By definition, incompatible elements such as H, Fe, Na and Al preferentially partition into a melt phase rather than remain in a solid phase, so partial melting events will deplete the SCLM of its incompatible elements. In contrast, metasomatism by fluids or melts that are enriched in incompatible elements (such as those released from a subducting slab or a plume) may re-fertilize it, so long as the interaction with the enriched fluids or melts is sufficiently slow that the incompatible elements begin to diffuse into the host rock (Hofmann 1997). Subduction transports (generally) oceanic crust, including sediments, into the mantle and takes with it species in which the crust is enriched that may be important controls on conductivity including C, Fe and H₂O (Plank and Langmuir 1998). The water transported by subduction zones occurs both as interstitial water in sediments, which will be squeezed out by pressure gradients at shallow depths, and as water bound in the structures of hydrous minerals, which will undergo dehydration reactions at appropriate pressure and temperature conditions (Moore and Vrolijk 1992; Stern 2002). Since the subducting slab is cold relative to the surrounding mantle, its temperature gradient is lower and the hydrous minerals will be able to remain stable to greater depths than would be possible in lithosphere with a normal geotherm. The majority of the dehydration reactions involved in subduction occur at depths <100 km, corresponding to the fore-arc and the arc on the surface of the over-riding plate (Stern 2002). However, water can be transported to much greater depths by serpentinite which may be stable to depths as great as 250 km (Ulmer and Trommsdorff 1995; Booker et al. 2004). While serpentinite is not expected to be conductive in its stable form (Guo et al. 2011; Reynard et al. 2011), it converts to olivine, orthopyroxene and water upon dehydration and will release as much as 13 wt% water, which is likely to increase the hydrogen content of surrounding NAMs. Demouchy (2010b) calculated that, for a typical mantle mineral aggregate, it would take 4 Gy for hydrogen to diffuse a distance of 14 km. Therefore, in the absence of melting or high-temperature events that would remove it, hydrogen will still be present in the lithosphere from enrichment events that occurred even several billion years ago.

Due to complicated phase equilibria, release of carbon from subducted rocks is more difficult to predict than water release (Stern 2002). Although the analysis of CO₂ emissions at arcs shows that the majority of the emitted carbon is from a subducted source (Marty and Tolstikhin 1998), calculations of phase equilibria show that much of the carbon in subducted rocks is likely to remain stable to depths greater than 180 km and will therefore be returned to the mantle (Kerrick and Connolly 1998, 2001a, b). Carbon from such depths is most likely to exist in the form of fluid inclusions in minerals and will not enhance conductivity (Mathez 1987). If carbon remains in fluid or vapor phases at temperatures lower than 600–900 °C, it may precipitate grain-boundary graphite films and increase conductivity by several orders of magnitude (Mathez 1987; Pineau and Mathez 1990; Glover 1996).

Mantle plumes have chemical signatures that are more enriched than the depleted upper mantle, although the degree and the nature of the enrichment show evidence for spatial variations (Hofmann 1997). Plumes are sourced from the asthenospheric mantle and are believed to come from either (or both) the 660-km seismic discontinuity or the core-mantle boundary (Hofmann 1997; Zhao 2001). Therefore, igneous rocks that are related to plume magmatism such as ocean island basalts and continental flood basalts demonstrate enrichment in incompatible elements, including iron (Dixon et al. 2002; Workman et al.

2006). Since the asthenosphere is likely to be more hydrous than the lithosphere (e.g., Karato 2006), lithospheric regions that have been impacted by a plume are also likely to have higher water contents. Given the large thermal impact of a plume, it is possible that resulting incompatible element patterns may be depth-dependent, with deep regions close to the plume head reaching sufficiently high temperatures to undergo partial melting and therefore becoming depleted while shallower regions that interact with the resulting melts become enriched.

3.6 General Comments

This analysis shows that, in general, as lithosphere ages and becomes cooler and more depleted in incompatible elements (including iron and hydrogen), it can be expected to become more resistive. However, it is not valid to consider this to be a universal rule. Lithosphere that has been compositionally affected by fluids or melts from a subducting slab or a plume will have a higher iron and hydrogen and carbon content than unmodified lithosphere and, as discussed above, these factors can cause an increase in conductivity in lithospheric rocks. The signature of enrichment from such an event may remain in the lithosphere for billions of years (Demouchy 2010a). Within the mantle, the range of iron contents is expected to be small and is likely to have a negligible impact on conductivity. In contrast, the possible differences in hydrogen concentrations, from close to zero to up to several hundred ppm, would be expected to change resistivity values by up to several orders of magnitude and have the potential to be a major influence on the conductivity structure of the lithosphere. Within the crust, the much larger ranges of iron content and higher iron values will lead to a measurable increase in conductivity in iron-rich regions. Carbon content will be of greater importance in the crust and uppermost mantle than in the deeper lithosphere since carbon is only likely to exist as grain-boundary graphite films at temperatures less than approximately 900 °C. Since the process of melting dehydrates and depletes the lithosphere, it is to be expected that regions that have experienced multiple melting episodes and have been subject to high temperatures will have low iron and hydrogen contents and no graphite films and will therefore be resistive. It is therefore likely that a younger (but still thermally stable) region that has undergone high-temperature events and has experienced voluminous melting will be more resistive than an older region that has been enriched by a subduction or a plume event at some point in its history but has been stable since. Figure 7 summarizes the different factors considered to control most resistivity anomalies in stable lithosphere and the depth ranges at which they are predicted to operate.

4 Case Studies

It is common for cratonic lithosphere to show lateral resistivity variations of several orders of magnitude which can often be related to specific enrichment or depletion events. Some cratonic lithosphere has high resistivities typical of standard lithospheric mineral compositions with little or no enrichment in Fe or H, that is crust and upper mantle resistivities of at least several thousand Ωm that decrease to several hundred Ωm toward the base of the lithosphere due to increasing temperature. Such regions include parts of the São Francisco Craton in Brazil (Bologna et al. 2011), the Dharwar Craton in India (Naganjaneyulu and Santosh 2012; Patro and Sarma 2009), the Kaapvaal Craton in South Africa (Evans et al. 2011) and the Superior and Slave Cratons in Canada (Ferguson et al. 2005; Jones et al.

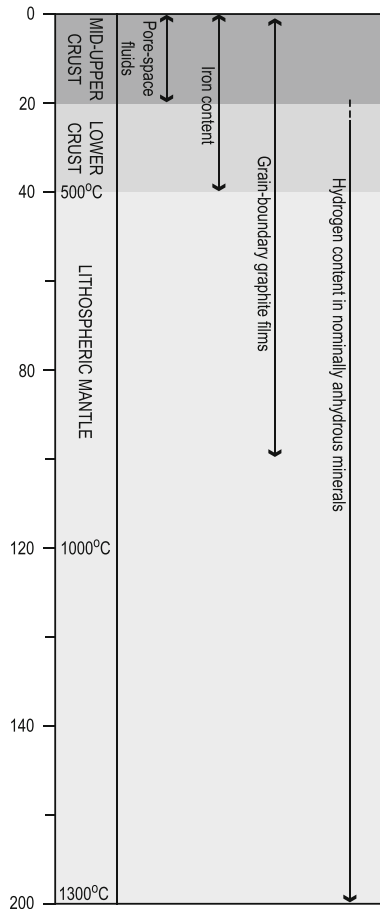


Fig. 7 Expected depth ranges for important causes of enhanced conductivity in the stable lithosphere. The thermal gradient is taken from the compilation of Artemieva (2006) assuming a lithospheric thickness of 200 km. Above the brittle–ductile transition in the crust, fluids may exist in interconnected pore spaces in sedimentary basins or in shear zones. The iron content of Fe/Mg-bearing minerals shows significant variation in the crust, and high iron contents are detectable as a conductive anomaly. Iron contents in the mantle are lower than the crust and show little variation. Grain-boundary graphite films have been shown experimentally to become disconnected at low pressures representative of the uppermost crust and to become unstable at temperatures greater than ~ 900 °C, corresponding to a depth of approximately 100 km. High hydrogen content in nominally anhydrous minerals has been shown to increase conductivity to depths greater than the base of the lithosphere. At the low-temperature end, hydrogen has been shown to enhance the conductivity of crustal rocks to mid-crustal depths (temperatures of 200–300 °C). The shallow limit of the effect of hydrogen will be defined by the lowest temperature at which hydrogen will diffuse

2005b). However, all of these cratons also contain much more conductive regions. Considering crustal examples first, a lower crustal conductor in the São Francisco Craton (~ 100 Ωm) has been interpreted to be caused by graphite and is associated with a proposed suture zone, the strongly conductive North America Central Plains (NACP) anomaly in central Canada (with resistivities <10 Ωm) is associated with interconnected sulfides at outcrop and a crustal conductor in the Dharwar Craton that is associated with gold mineralization has also been interpreted to be caused by sulfides (Gokarn et al. 2004). In the

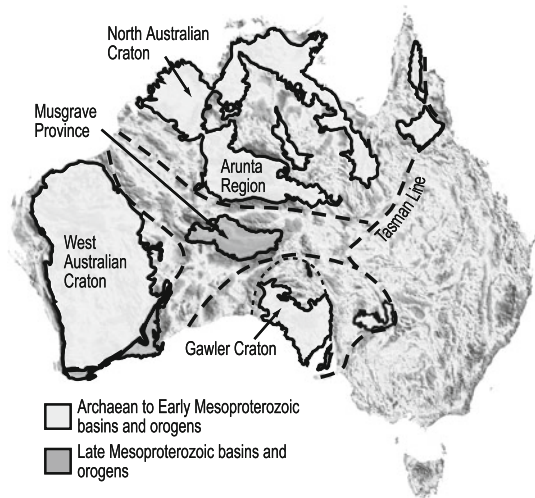
lithospheric mantle, cratonic low-resistivity regions are also common. In the São Francisco Craton and neighboring Proterozoic Brasilia Belt, a region with resistivities as low as $1 \Omega\text{m}$ that extends to the lower lithosphere has been interpreted to be caused by graphite and incipient carbonatite melting (Bologna et al. 2011; Figueiredo et al. 2008), while other upper mantle regions with resistivities of $\sim 100 \Omega\text{m}$ are interpreted to be due to iron enrichment of mantle minerals (Bologna et al. 2011). In the northwestern Dharwar Craton, a low-resistivity region ($\sim 100 \Omega\text{m}$) extends through the upper mantle to a depth of $\sim 50 \text{ km}$ (Gokarn et al. 2004) with a genesis that could possibly be related to the Deccan Traps, a c. 66 Ma large igneous province to the north of the survey location. The SCLM of the Archean Churchill Province in western Canada is an order of magnitude more conductive (at several hundred Ωm) than that of the surrounding Proterozoic terranes, interpreted to be due to fertilization of the Archean lithosphere during subduction-related metasomatism in the Paleoproterozoic (Boerner et al. 1999). Beneath the NACP anomaly in central Canada, a region with resistivities of tens of Ωm extends to the limit of data resolution in the mantle and has been interpreted to be related to nearby diamond-bearing kimberlites (Jones et al. 2005a). The Bushveld Complex, a large, Paleoproterozoic layered igneous intrusion in the Kaapvaal Craton, is extremely conductive, with resistivities as low as $\sim 1 \Omega\text{m}$ centered in the lower crust and at 60–85 km depth and all mantle resistivities significantly less than $100 \Omega\text{m}$. It has been suggested that a combination of sulfides associated with the Bushveld Complex intrusion with pre-existing Fe-rich or graphite-rich country rocks could explain these very low resistivities (Evans et al. 2011).

The Dharwar, Slave, Kaapvaal and São Francisco Cratons (among others) all demonstrate lateral conductivity gradients of two to three orders of magnitude and show that it is fallacious to simply consider Archean cratons to be resistive. While it is not possible to closely analyze each cratonic MT survey, it is informative to consider case studies of two representative regions of stable lithosphere in Australia and Canada that characterize the different resistivity factors described above. Recent work by Fullea et al. (2011) is an excellent example of a detailed, numerical calculation of the combined effects of temperature, mineralogy, composition and hydrogen content and comparison to MT data. Such a detailed analysis is beyond the scope of this paper and, in many instances, requires better-quality MT, geological and thermal data than are available. Instead, the focus will be on the broadly expected resistivities for both anhydrous and hydrous compositions in the regional geothermal regimes to examine correlations between conductivity, temperature and enrichment.

4.1 Case Study 1: The Gawler Craton and Musgrave Block, Australia

Central and western Australia is composed of Archean to Paleoproterozoic cratons that are separated by Mesoproterozoic to Neoproterozoic orogens (Fig. 8) (Betts et al. 2002). Due primarily to a paucity of outcrop within Precambrian Australia, there is significant uncertainty about the timing and location of collisions between cratonic elements and the nature of the younger regions. This has been the motivation for many of the MT surveys in the region (e.g., Selway et al. 2009b, 2011; Thiel and Heinson 2010; Heinson et al. 2006), but the lack of geological information that motivated these surveys has in turn also hampered their interpretation. In light of the above discussion, MT results from the Archean to Paleoproterozoic Gawler Craton in southern Australia, the Paleoproterozoic Arunta Region in northern Australia and the Mesoproterozoic to Neoproterozoic Musgrave Block in central Australia will be examined to determine whether the mapped conductivity structures correspond with known thermal, compositional and enrichment patterns.

Fig. 8 Cratonic regions within Australia. The Mesoproterozoic to Neoproterozoic Musgrave Province in central Australia is surrounded by the Archean to Paleoproterozoic Gawler Craton to the south, the North Australian Craton (including the Paleoproterozoic Arunta Region) to the north and the West Australian Craton to the west. The lithosphere to the east of the Tasman Line is Phanerozoic in age



4.1.1 Gawler Craton

The Gawler Craton, South Australia (Fig. 9) (Hand et al. 2007), consists of a Mesoarchaean to early Palaeoproterozoic core that is overlain and intruded by Palaeo- to Mesoproterozoic lithologies (Daly et al. 1998; Hand et al. 2007; Payne et al. 2009). The Archean nucleus consists of the Neoarchaean Mulgathing and Sleaford Complexes, which are dominated by sedimentary, volcanic and plutonic rocks that were deformed and metamorphosed during the ca. 2,470–2,430 Ma Sleafordian Orogeny (McFarlane 2006; Swain et al. 2005; Tomkins and Mavrogenes 2002). Recently discovered Mesoarchaean, c. 3,150 Ma felsic gneisses are likely to form the basement to these Neoarchaean complexes (Fraser et al. 2010). To the east and the north of the Archean core are a series of Palaeoproterozoic igneous intrusives and volcano-sedimentary basins that have been variably metamorphosed throughout the Proterozoic (Daly et al. 1998; Hand et al. 2007; Howard et al. 2009; Payne et al. 2006, 2008; Chalmers 2007; Fanning et al. 2007; Forbes et al. 2012). Isotopic evidence suggests that much of the Gawler Craton that is defined as Proterozoic based on surface geology is underlain by Archean lithosphere (Fanning et al. 2007; Hopper 2001).

As discussed above, metasomatism by enriched fluids from a subducting slab or a plume will re-fertilize Archean lithosphere in incompatible elements (including hydrogen) and increase its conductivity. Australian Precambrian lithosphere is conspicuous for showing very little evidence of subduction-related processes, but the Paleoproterozoic 1,620–1,608 Ma St Peter Suite in the southwest of the Gawler Craton is one package that has been interpreted as having formed in a subduction-related environment (Swain et al. 2008). The St Peter Suite displays enriched incompatible element compositions, including Ce and Nd that are expected to have similar incompatibilities to hydrogen (Michael 1988), and is interpreted to have originally formed as an island arc that later accreted to the Gawler Craton (Swain et al. 2008). Swain et al. (2008) interpret that the subduction zone that formed the St Peter Suite dipped away from the Gawler Craton, so it would not be expected that deep lithospheric zones of enrichment would exist below the St Peter Suite but it is possible that shallower zones of enrichment in the lower crust and uppermost mantle may have been preserved during its accretion. Following the emplacement of the St Peter Suite,

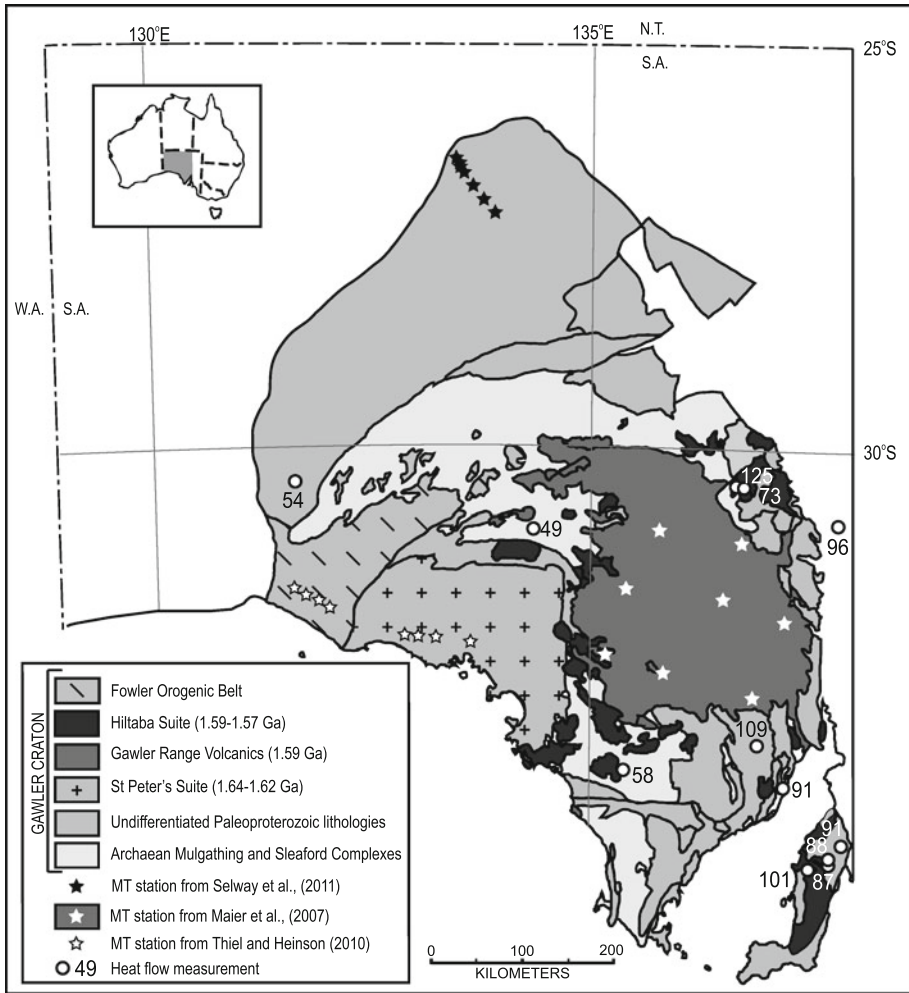


Fig. 9 Simplified map of the Gawler Craton, South Australia, showing the geological regions discussed in the text. *Labelled circles* show surface heat flow measurements from Neumann et al. (2000). *Stars* show the locations of MT stations used in the analysis. *Black stars* are stations in the Proterozoic northern Gawler Craton from Selway et al. (2011), *white stars* are stations on the Gawler Range Volcanics from Maier et al. (2007), and *white stars with black outline* are stations on the Proterozoic western Gawler Craton and the St Peter Suite from Thiel and Heinson (2010)

the Gawler Range Volcanics (GRV) and associated Hiltaba Suite granitoids were extruded between 1,595 and 1,575 Ma either as a result of a plume impact or formation in a back-arc basin setting (Betts et al. 2009). The GRV (Allen et al. 2008) is a felsic large igneous province (LIP) that occupies a volume of at least 25,000 km³ in the center of the Gawler Craton. Since it is a felsic unit, it is derived from crustal melting and its enriched composition (Allen et al. 2008) does not provide any information about the fertilization state of the underlying mantle. The Hiltaba Suite (Stewart and Foden 2003) is also dominantly felsic but does contain a minor mafic component. Isotopic variations within the Hiltaba Suite have been interpreted to suggest that it was derived from a depleted mantle source mixed with a

crustal component (Hand et al. 2007). Either of the proposed formation mechanisms (plume or back-arc basin) would result in the enrichment of the lithosphere so the upper mantle beneath the GRV/Hiltaba Suite would be expected to have a higher conductivity than that expected for dry lithosphere. Since there have been no major tectonothermal events in the Gawler Craton since the emplacement of the GRV/Hiltaba Suite (Allen et al. 2008), this region of enrichment would be expected to remain today.

In contrast to the global average thermal regimes discussed above, southern and central Australia has an anomalously high heat flow (Cull 1982; McLaren et al. 2005) with a mean of heat flow measurements in South Australia 86 ± 20 mW/m² (Fig. 9) (Neumann et al. 2000). This high heat production is interpreted to be caused by high heat-producing (HHP) elements such as U, Th and K that lie predominantly in the upper crust (McLaren et al. 2005; Neumann et al. 2000) and are therefore not expected to cause any significant increases to mantle temperatures (McKenzie et al. 2005; McLaren et al. 2005). Therefore, despite anomalous surface heat flow values, mantle conductivities are not expected to be thermally enhanced.

Thiel and Heinson (2010) reported results of an MT survey to a depth of 200 km over the western Eyre Peninsula region of the Gawler Craton that crossed from the subduction-related St Peter Suite westwards over the Paleoproterozoic Fowler Domain (Fig. 9). The geology of the Fowler Domain is very poorly understood and is entirely constrained by interpretations of potential field data and analysis of samples from rare drill core (Howard et al. 2011). However, near-surface metasedimentary rocks have reached high metamorphic grades up to granulite facies and show affinities with other metasedimentary packages from the Gawler Craton, suggesting that they were not involved in any collisional orogenesis (Howard et al. 2011). Results from the MT survey show that, beneath a shallow conductive layer which is probably due to interconnected pore fluids in the upper crust, the bulk of the imaged lithosphere has very high resistivities between 10^4 and $>10^5$ Ω m, which is in the range of expected resistivities for dry, depleted lithosphere at the temperature conditions of the western Gawler Craton (Fig. 10). In contrast, the crust and upper mantle beneath the St Peter Suite display some zones of decreased resistivity, to values of one hundred to several hundred Ω m at depths up to approximately 60 km (Fig. 10). These resistivity values cannot be explained by dry lithosphere in the thermal regime of the western Gawler Craton and show that there must be an additional component present to enhance conductivity. Given the depth range of the conductive zone and the fact that it lies beneath the subduction-related St Peter Suite, it is likely that the conductivity is enhanced by either (or both) an increased hydrogen content in lower crustal and upper mantle NAMs that was produced during dehydration of subducted hydrous minerals or graphite films on grain boundaries caused by precipitation of subducted carbon.

There are no published two-dimensional MT models that cross the GRV but Maier et al. (2007) published one-dimensional resistivity-depth profiles from a group of long-period MT stations that were deployed on the GRV (Fig. 9). Resistivities in the crust increase from several tens of Ω m at the top of the crust to several hundreds of Ω m at its base. In the lithospheric mantle, all stations show a pronounced low-resistivity zone of <100 Ω m at approximately 60–70 km depth, before resistivity increases slightly to 100–300 Ω m at 100–200 km depth (Fig. 10). This lithosphere is therefore conductive compared to what would be expected for dry, depleted lithosphere. Even though this region has elevated surface heat flow compared to the global reference model, it is not expected to have elevated lithospheric temperatures and a temperature increase approaching 1,000 °C would be required to account for the modelled resistivities, which is clearly unrealistic. Instead, lithospheric resistivity must again be enhanced by increased hydrogen content in NAMs

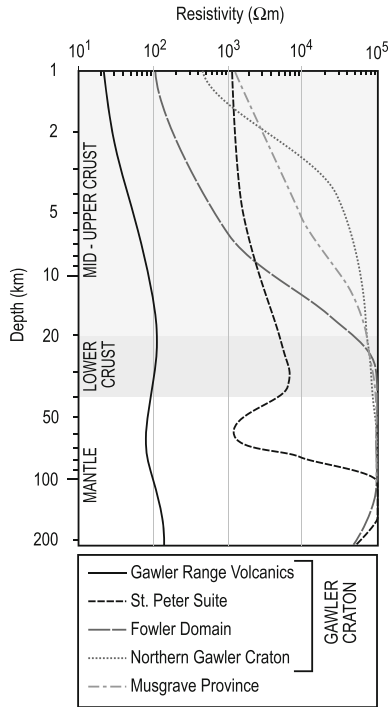


Fig. 10 Resistivity depth slices for the Gawler Range Volcanics (GRV) in the central Gawler Craton (Maier et al. 2007), the Paleoproterozoic Fowler Domain on the western Gawler Craton (Thiel and Heinson 2010), the Paleoproterozoic, subduction-related St Peter Suite on the western Gawler Craton (Thiel and Heinson 2010), the Paleoproterozoic northern Gawler Craton (Selway et al. 2011) and the Mesoproterozoic Musgrave Province in central Australia (Selway et al. 2011), shown to a maximum resistivity of $10^5 \Omega\text{m}$. The depth slice for the GRV is taken from one-dimensional modelling in Maier et al. (2007), while the other slices are averaged from two-dimensional models. All regions show moderate and variable resistivity in the mid- to upper crust which could be due to fluids or conductive minerals. In the lower crust and upper mantle, resistivities lower than those expected for hydrogen- and graphite-free minerals are only evident for the GRV and the St Peter Suite. These lithologies are associated with re-fertilization of the lithosphere, which is expected to enrich the lower crust and lithospheric mantle in hydrogen and potentially deposit graphite films. Although the Musgrave Province is younger than the Gawler Craton, it demonstrates high resistivities because numerous high-temperature tectonothermal events have removed hydrogen and carbon from the lithosphere

and/or graphite films on grain boundaries. The conductive anomaly extends to at least 200 km depth, which is greater than the depth to which grain-boundary graphite films will be stable. Therefore, at least some of the enhanced conductivity must be due to hydrogen in NAMs. At shallower levels, graphite films could contribute to the enhanced conductivity. Indeed, experimental data do not show evidence of hydrated mantle minerals reaching resistivities as low as those observed in the low-resistivity zone at 60–70 km depth, so it is likely that graphite films contribute to the enhanced conductivity at this level and it is possible that the marked decrease in resistivity in this zone corresponds with the appearance of grain-boundary graphite films.

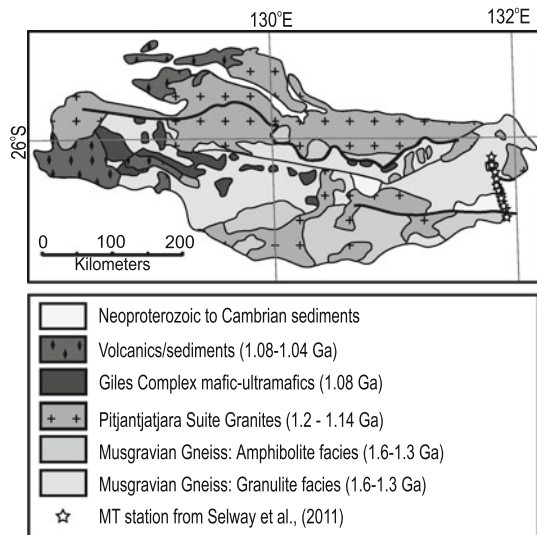
Figure 10 shows a comparison of resistivity-depth profiles from the GRV ((Maier et al. 2007), the Fowler Domain (Thiel and Heinson 2010), the St Peter Suite (Thiel and Heinson 2010) and the far-northern Gawler Craton (Selway et al. 2011). The SCLM of the regions

not expected to show any signs of re-fertilization, that is, the Fowler Domain, the deep lithospheric mantle beneath the St Peter Suite and the far-northern Gawler Craton, demonstrates resistivities between 10^4 and $10^5 \Omega\text{m}$. In contrast, the entire lithospheric column beneath the GRV and the lower crust and uppermost mantle beneath the St Peter Suite demonstrate much lower resistivities, showing a correlation between surface geology that indicates lithospheric enrichment and conductive lithosphere.

4.1.2 Musgrave Province

The Musgrave Province (Fig. 11) (Wade et al. 2008) is enigmatic in that it is a comparatively young and isotopically juvenile region that is surrounded by much older, more evolved cratons. The oldest known rock package in the Musgrave Province is the Mesoproterozoic, 1,600–1,540 Ma Musgravian Gneiss, which has geochemical characteristics suggesting it was formed in a subduction-related arc environment, interpreted to be related to the collision between the Gawler Craton to the south and the North Australia Craton to the north (Wade et al. 2006). Following a period of sedimentation, the Musgrave Province was deformed by the high-grade, 1,230–1,150 Ma Musgrave Orogeny which is represented by regional amphibolite to granulite-grade mineral assemblages in currently exposed surface rocks. The Musgrave Orogen has recently been recognized to extend into the southern Arunta region, more than 200 km north of the most northerly exposed section of Musgrave Province (Morrissey et al. 2011). This high-temperature event was associated with emplacement of the granitic, c. 1,200–1,140 Ma Pitjantjatjara Supersuite which is volumetrically dominant in the northern Musgrave Province and enriched in U and Th. The 1,080–1,040 Ma Giles Event was a deformational event associated with the emplacement of layered mafic-ultramafic dykes, felsic dykes and bi-modal volcanics of the Giles Complex. Coeval dyke emplacement over a large area of western and northern Australia led Wingate et al. (2004) to interpret that the dykes formed in response to the interaction between the lithosphere and a mantle plume. Following the Giles Event, emplacement of dykes continued and the Alcurra and Amata dykes were emplaced from 1,080–820 Ma.

Fig. 11 Simplified geological map of the Musgrave Province, central Australia, showing the lithological units discussed in the text, adapted from Wade et al. (2008). Stars show the locations of MT stations from Selway et al. (2011) that were used in the analysis



From c. 630–530 Ma, the Musgrave Province was metamorphosed and deformed by the Petermann Orogeny. This was an intracratonic event that occurred in response to far-field forces thought to have been localized in this region partly because initial crustal temperatures were elevated by high crustal heat production (Hand and Sandiford 1999). The metamorphic grade of the orogen reaches granulite grade in the northern Musgrave Province and sub-eclogite grade in the center of the Province, where the high-grade rocks were exhumed from an estimated depth of 45 km (Wade et al. 2008; Scrimgeour and Close 1999).

The Musgrave Province therefore displays a complex sequence of events that could be expected to affect the enrichment, hydrogen content and graphite content of the lithosphere. The original subduction event that created the arc-related Musgravian Gneiss would have been likely to result in a lithosphere containing significant hydrogen in NAMs and possible grain-boundary graphite films. However, the high temperatures reached during the Musgrave Orogeny would have removed much of this material from the lithosphere. Rocks currently at the surface reached temperatures between 750 and >900 °C during the Musgrave Orogeny (Wade et al. 2008), so at any greater depth, graphite films would have become unstable and incompatible elements would have been partitioned into the Pitjantjatjara Supersuite. The two interpreted plume events would also be expected to enrich the lithosphere, but geochemical data suggest that this enrichment may have only been minor. Geochemical signatures from both the Giles Complex and Amata dykes show only a moderate enrichment in incompatible elements compared to MORB. Ce and Nd, which behave similarly to hydrogen, are only enriched by approximately 2–3 times over MORB in dykes of the Giles Complex in the western Musgrave Province (Wingate et al. 2004) and in Amata dykes (Zhao et al. 1994). Rocks currently exposed at the surface reached temperatures of 650–750 °C during the Petermann Orogeny (Wade et al. 2008). Such high-temperature metamorphism is likely to have liberated some or most of the incompatible elements emplaced in the lithosphere during the plume events and destroyed any grain-boundary graphite films at depths greater than the mid-crust.

MT surveys over the Musgrave Province show that the lithosphere is uniformly highly resistive. Selway et al. (2011) describe results of a profile extending from the northern Gawler Craton into the southern Musgrave Province (Fig. 11). Apart from a shallow zone restricted to the upper crust with resistivities as low as 10 Ωm, the entire lithospheric section displays resistivities >10⁴–10⁵ Ωm to the modelled depth of 100 km (Fig. 10). The southern Musgrave Province was analyzed to be approximately electrically one-dimensional, and forward modelling suggested that there were no major conductive features further north within the province (Selway et al. 2011). Similarly high-resistivity lithosphere has been imaged elsewhere in the Musgrave Province. The northern Musgrave Province lithosphere, together with the lithosphere beneath the Amadeus Basin and in the southernmost Arunta Region to its north, is resistive compared to the more northerly Arunta Region (Selway et al. 2009a). This region of high resistivity is spatially coincident with the Musgrave Orogen. The absolute values of resistivity in the north are lower than those described in the southern Musgrave Province, at approximately 3 × 10³–10⁵ Ωm, but these values may be elevated by smoothing of the conductive signal associated with the Amadeus Basin. Indeed, resistivity values of approximately 10⁵ Ωm are observed in the southern Arunta Region, which is not overlain by the Amadeus Basin (Selway et al. 2009a). Sub-cropping rocks of the northern Musgrave Province were imaged to a depth of only 1 km by Selway et al. (2012) and had a resistivity of 10⁴ Ωm. A survey across the western Musgrave Province has also shown the lithosphere to be highly resistive, with modelled resistivities greater than 10⁴–10⁵ Ωm (M. Dentith, pers. comm., 2012).

The resistivities observed in the Musgrave Province are all representative of dry lithosphere with no additional conductive component. This shows that, even though the lithosphere has been affected by subduction and possibly two plume events, the very high-grade metamorphic events that have subsequently affected the Musgrave Province have removed any introduced hydrogen and carbon from the lithosphere. This behavior contrasts with that observed in the lithosphere beneath the GRV in the Gawler Craton. That region was impinged upon by a plume (or a subduction zone) that introduced conductive elements to the lithosphere but has been stable since, so the lithosphere remains conductive. It is the tectonically stable, cratonic nature of this region that has enabled this conductive signature to remain in the lithosphere for over 1.5 billion years. In contrast, the Mesoproterozoic to Neoproterozoic Musgrave Province is a much younger “mobile belt” that has experienced multiple episodes of tectonism and would often be expected to have a lower resistivity. However, it is the very tectonic instability of the Musgrave Province that has removed any introduced hydrogen and carbon and has resulted in such a high-resistivity lithosphere. Therefore, it is important to consider not only the age of the lithosphere being imaged but whether it has experienced any enrichment events and, if so, whether that signature is likely to remain.

4.2 Case Study 2: The Slave Craton, Canada

The Slave Craton (Fig. 12) (Davis et al. 2003) is a small, Archean Craton in central-northern Canada that is surrounded by Palaeoproterozoic orogenic belts. The basement of the western Slave Craton is dominated by the c. 4.0–2.9 Ga Central Slave Basement Complex, while the central and eastern Slave Craton display younger, <2.8 Ga, isotopically juvenile crust that is enriched in Pb and Nd (Davis et al. 2003 and references therein). Intruding the Archean basement rocks of the central and eastern Slave Craton are a 2.73–2.7 Ga tholeiitic volcanic sequence and a voluminous mafic magmatic sequence that shows affinities to modern LIPs and may suggest a mantle plume source (Davis et al. 2003). This was followed by widespread calc-alkaline volcanism from 2.7 to 2.66 Ga in the eastern and the western Slave Craton. Two major tectonothermal events affected the craton between 2,640 and 2,585 Ma and involved horizontal shortening and metamorphism up to granulite facies. This tectonism was associated with two episodes of plutonism; the first produced >2,620–2,600 Ma granites that are interpreted to be sourced from a subduction-enriched mantle and the second involved a craton-wide 2,610–2,585 Ma “granite bloom” which suggests that there was a large thermal disturbance to the mantle at that time, possibly in the form of lithospheric delamination, post-collisional extension or interaction with a mantle plume (Davis et al. 2003 and references therein). During the Proterozoic, the region was intruded by numerous dyke swarms, including at 2,230, 2,210, 2,190–2,180, 2,108, 2,030–2,023, 1,884 and 1,272–1,265 Ma (Heaman and Pearson 2010 and references therein). Numerous kimberlites have intruded the craton within the last ~ 500 Myr, including the Ekati cluster (53 Ma) and Diavik cluster (55 Ma) in the central Slave Craton, the Jericho kimberlite (172 Ma) in the northern Slave Craton, the Drybones Bay kimberlite (440 Ma) in the western Slave Craton and the Gahcho Kue kimberlite (530 Ma) in the southeastern Slave Craton (Heaman and Pearson 2010 and references therein).

The voluminous kimberlites throughout the Slave Craton have brought to the surface numerous mantle xenoliths that point to a complex mantle history. Although the surface geology of the Slave Craton is dominated by Archean rocks, analysis of Re–Os ages for the Slave mantle xenoliths indicates that only approximately 30 % of them were formed

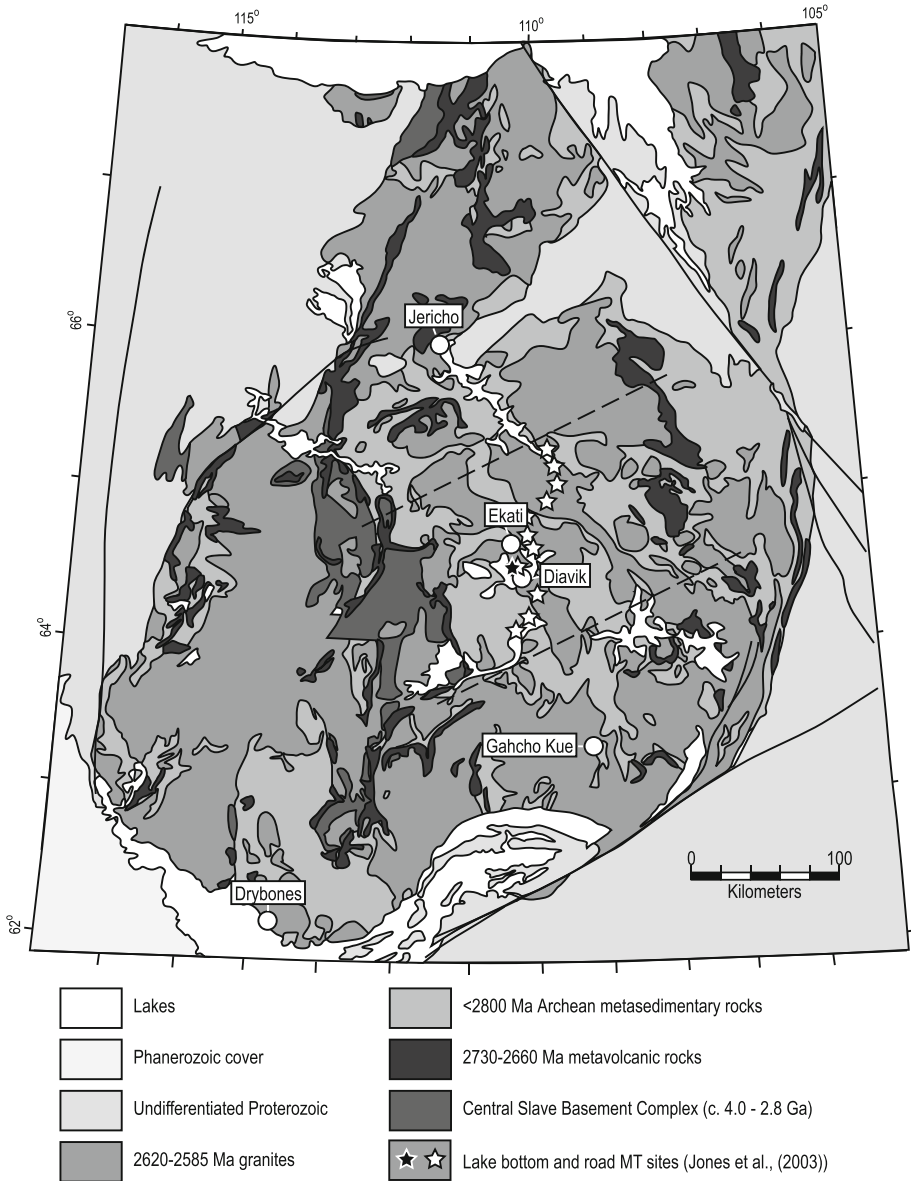


Fig. 12 Simplified geological map of the Slave Craton, Canada, showing the lithological units discussed in the text, adapted from Davis et al. (2003) and Heaman and Pearson (2010). Between the dashed lines is the region containing sub-calcic garnets defined by Grütter et al. (1999). *Filled circles* show the locations of the xenolith suites that have undergone significant analysis. *Stars* show the locations of MT stations from Jones et al. (2001, 2003) that are used in further analysis. *White stars with a black outline* are stations deployed on roads, while the *black star with a white outline* is a station deployed on the bottom of Lac de Gras which provides deeper-penetrating data

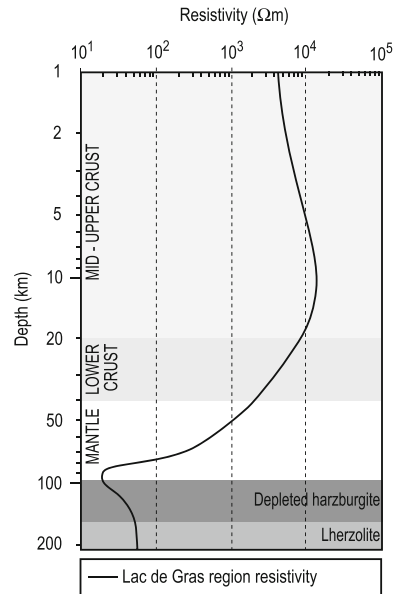
during the Archean and the bulk of the mantle formed during the Proterozoic (Heaman and Pearson 2010). Peaks in interpreted mantle formation ages are at 2.75 Ga (interpreted to correspond to the formation of the central and eastern Slave crust), 1.8 Ga (interpreted to

correspond to accretion of subducted lithosphere from the Wopmay Orogen to the west), 1.3 Ga (interpreted to correspond to emplacement of the Mackenzie LIP in the northern Slave Craton) and a minor peak at 0.4 Ga which may be related to the Drybones Bay kimberlite (Heaman and Pearson 2010 and references therein). Geochemical and isotopic analysis of xenoliths shows extensive evidence of metasomatism and re-fertilization throughout the craton with significant lateral variation in depth, age and character (Aulbach et al. 2007; Davis et al. 2003; Griffin et al. 2004; Heaman and Pearson 2010). The lithospheric mantle of the central Slave Craton is sampled by the Lac de Gras kimberlites, which show two distinct compositional layers. An upper layer, representing xenoliths from $\sim \leq 95$ depth to ~ 145 km depth, is characterized by harzburgites with highly depleted geochemical signatures and high Mg#, whereas a lower layer, from ~ 145 to $\sim \geq 155$ km depth is characterized by harzburgites and lherzolites with a more enriched geochemical signature and lower Mg# (Griffin et al. 1999; Aulbach et al. 2007; Pearson et al. 1999). The uppermost, depleted layer was originally interpreted as anomalously ultra-depleted (Griffin et al. 1999), but a more recent interpretation (Griffin et al. 2009) suggests that it is instead characteristic of Archean lithosphere that has not been re-fertilized through younger processes. In contrast, the deeper layer in the central Slave SCLM and the bulk of the sampled SCLM in the northern, eastern and western Slave show evidence for re-fertilization due to enriched incompatible element concentrations and elevated iron contents (Davis et al. 2003; Griffin et al. 2004; Heaman and Pearson 2010). Given this, it would be reasonable to expect that the upper lithosphere of the central Slave Craton lithosphere would demonstrate the high resistivities expected for dry, depleted lithosphere and the lower lithosphere should demonstrate lower resistivities.

Jones et al. (2001, 2003) describe results from MT surveys through the southern and central Slave Craton (Fig. 12). A one-dimensional model created by averaging the resistivities of all stations on the craton suggests that below a resistive lower crust, the lithospheric mantle displays resistivities of 10^2 – 10^3 Ωm and is therefore more conductive than dry, graphite-free lithosphere. One-dimensional and two-dimensional modelling has imaged a very low-resistivity zone in the central Slave Craton, termed the Central Slave Mantle Conductor (CSMC). Two-dimensional modelling shows that the depth to the top of the CSMC increases from ~ 80 km at its northern extent to ~ 100 km at its southern extent, and integrations of its conductance suggest that it is best fit by a zone of resistivity ≤ 30 Ωm and thickness ~ 25 km (Fig. 13) (Jones et al. 2003). Due to the high conductivity of this zone, much of the MT signal is attenuated within it and the only data that penetrate through it are from one very long-period, lake-bottom site. These data show that the resistivity of the lithosphere increases below the CSMC but remains at values of ~ 50 Ωm . The exceptionally low resistivities are only observed at the CSMC, but the two-dimensional modelling shows that much of the rest of the modelled Slave Craton lithospheric mantle has resistivities in the order of several hundred to several thousand Ωm (Jones et al. 2003).

Jones et al. (2001, 2003) interpret the cause of the low resistivity in the CSMC to be grain-boundary graphite films, noting that the resistivity is too low to be caused purely by hydrogen, but consider that the enhanced conductivity at greater depths (and outside the stability field of graphite) may be due to hydrogen diffusion. The authors note the apparent spatial correspondence between the CSMC and the depleted harzburgite layer (Griffin et al. 1999), a geochemically defined zone of sub-calcic garnets that also imply high levels of depletion (Fig. 12) (Grütter et al. 1999) and the zone of Eocene-aged kimberlite emplacement (Fig. 13). They interpret that the sub-calcic garnet zone is related to the enhanced conductivity and suggest that the graphite films were formed during imbrication

Fig. 13 Resistivity-depth section of the MT data of Jones et al. (2001, 2003) through the Lac de Gras region of the Slave Craton. The shallowest xenoliths from the depleted harzburgite layer are from approximately 95 km depth, and the boundary with the underlying lherzolitic layer is at 145 km depth



of subducted slabs onto the base of the lithosphere at c. 2,630 Ma (Davis et al. 2003; Chen et al. 2009). However, from the analysis presented in this review, the interpretation that a high conductivity zone is genetically associated with a geochemically depleted zone is problematic. By definition, depleted zones are depleted in hydrogen and carbon that could cause enhanced conductivity. Additionally, during the interpreted imbrication, metamorphic temperatures at c. 2,600 Ma were >700 °C at the base of the crust, making it unlikely that temperatures at depths of 80–120 km would have been low enough for graphite films to be stable.

An alternative explanation for the genesis of the CSMC is that, rather than being related to Archean zones of depletion, it is related to younger patterns of kimberlite emplacement. Kimberlites are often spatially and temporally associated with carbonatites (Haggerty 1994). The Lac de Gras kimberlites in the central Slave Craton contain carbon-rich fluid inclusions, showing that the source region for the melts in the lower lithosphere or upper asthenosphere contained carbon (van Acherbergh et al. 2004). Metamorphic phase equilibria show that much of the carbon in carbon-rich kimberlites will be released as a vapor or a melt at depths of approximately 80–100 km (Wyllie 1980; Hunter and McKenzie 1989), with a characteristic interstitial angle sufficiently low to allow it to move along grain boundaries (Hunter and McKenzie 1989). Since this behavior of carbon can produce grain-boundary graphite films (Mathez 1987; Mathez et al. 1984), it is expected that the kimberlites that brought deep carbon to the surface in the Lac de Gras region would also produce grain-boundary graphite films in the depth range 80–100 km, as observed. The original source of the carbon that forms the graphite films may indeed have been early subduction since much of the carbon associated with the Lac de Gras kimberlites was sourced from subducted sediments (van Acherbergh et al. 2002). However, the high-temperature metamorphism and voluminous magmatism that has affected the central Slave Craton since the Archean shows that it is not plausible for grain-boundary graphite films to have formed during these ancient subduction events and subsequently survived in the upper mantle since that time. Instead, the carbon from the ancient subduction was stored in the

lower lithosphere or upper asthenosphere and later re-mobilized by kimberlite emplacement at c. 55 Ma to form the grain-boundary graphite films. This interpretation also removes the need for contentious Paleoproterozoic subduction in the Slave Craton that Chen et al. (2009) proposed, following from their interpretation that the genesis of the graphite films was associated with the genesis of the depleted harzburgite layer. Since graphite films would not have survived from the Paleoproterozoic and the carbon is more likely to have been re-mobilized from deeper in the lithosphere, it is not relevant to interpret the age of subduction events from the age of the formation of the harzburgite layer. Importantly, this interpretation also removes the genetic association between the CSMC and the depleted mantle layer, which is difficult to reconcile with the known behavior of hydrogen and carbon.

It is unknown whether the grain-boundary graphite films are on minerals in the depleted harzburgite layer or a different lithological unit. The shallowest depleted harzburgite xenoliths from the Ekati and Diavik pipes are from 95 km depth (Griffin et al. 2004) which is slightly deeper than the estimated depth extent of the CSMC at this location (Fig. 13) (e.g., Chen et al. 2009). Therefore, it is possible that the graphite-film deposition occurred in a layer shallower than the depleted harzburgite. However, it is also possible that graphite films deposited in the harzburgite layer are not represented in xenolith samples due to timing of extraction or destruction of the films during eruption. Any section of depleted harzburgite not affected by grain-boundary graphite films would be expected to be highly resistive, but resolution of the MT data beneath the CSMC is poor and it is questionable whether a thin, high-resistivity layer would be resolvable. The generally low-resistivity values observed throughout the Slave Craton lithosphere are interpreted to be due to hydrogen introduced into the lithosphere during the numerous subduction-related and plume-related re-fertilization events.

5 Discussion

The analysis presented in this review suggests that, in general, the resistivity of stable continental lithosphere will be related to its level of enrichment in incompatible elements. This assertion has important implications both for MT data interpretation and for improving our understanding of the lithosphere.

In interpreting MT data, the simple paradigm which states that Archean, cratonic lithosphere should be more resistive than Proterozoic or younger lithosphere should not be relied upon. Conduction in stable lithosphere of any age will be determined primarily by its temperature, the presence of hydrogen in NAMs and the presence of grain-boundary graphite films. Each individual region being surveyed should be considered independently for each of these factors. On average, Archean lithosphere has experienced more high-temperature events which will melt mantle rocks and remove hydrogen and destroy grain-boundary graphite films than younger lithosphere. However, the examples shown from the Gawler Craton, Musgrave Province and Slave Craton show that this is not universally true. A subduction or plume event may have introduced hydrogen and carbon into Archean lithosphere as much as several billion years ago and, if no subsequent high-temperature events have occurred to remove those species, they will remain to produce a conductive anomaly. In contrast, younger lithosphere may have experienced numerous high-temperature events that will result in it having low hydrogen content in NAMs, no grain-boundary graphite films and a high resistivity.

The possibility that MT can image regions of enrichment in incompatible elements in the lithosphere has important implications for interpreting lithospheric structure and

evolution. As described by Griffin et al. (2009), even in those few regions where mantle xenoliths are available, inferred SCLM compositions are often biased by sampling and by the tectonic environments likely to produce xenoliths. The idea that hydrogen in NAMs can be used as a broad proxy for enrichment in other incompatible elements raises the possibility that MT can be used to “map” the enrichment state of the lithosphere. This can be useful for developing our understanding of many geological processes such as the relationship between crustal and mantle evolution, lithospheric rheology and the growth and stabilization of cratonic lithosphere (Hirth and Kohlstedt 1996; Karato and Wu 1993) as well as for interpreting geological histories of specific regions. In addition, many styles of ore deposit require a lithosphere that is enriched in incompatible elements to form (e.g., Hedenquist and Lowenstern 1994; Ohmoto 1986) and the ability to map these zones of enrichment in the lithospheric mantle may assist in identifying prospective areas for mineral exploration.

6 Conclusions

MT studies, regardless of their resolution or depth penetration, can only provide a measure of one physical property of the Earth: its electrical resistivity. To make meaningful interpretations of MT data, it is necessary to combine MT results with an understanding of the mineralogical features that control resistivity and the geological processes that produce those mineralogies. While melt and fluid can produce conductive anomalies in tectonically active lithosphere, such features are not expected to be present in tectonically stable lithosphere. Instead, results from a growing body of mineral physics data show that in stable tectonic regimes, resistivity will be controlled primarily by temperature and mineral composition and that the most important compositional factor is hydrogen content in nominally anhydrous minerals (NAMs). Iron content in (Fe, Mg) silicates can also be an important factor in the crust, but the range of iron contents in mantle minerals is sufficiently small that it will not have a measureable effect on most MT results. In contrast, hydrogen content is an important variable from at least the mid-crust to the asthenosphere. Graphite films on the grain boundaries of minerals will also dramatically increase conductivity but are only stable from the crust to uppermost mantle temperatures of approximately 900 °C.

In seeking to make geological interpretations from MT data, several of the variables that can affect conductivity are often known. The thermal regimes of stable lithosphere are generally well understood and can be further constrained by utilizing heat flow data from the region being investigated. Furthermore, mineral proportions and iron content of the SCLM change systematically with lithospheric tectonic age. In most cases, the only two unknown variables that could dramatically influence electrical conductivity in tectonically stable regions are the presence of grain-boundary graphite films and hydrogen content in NAMs. Both of these species will be controlled by past tectonic events in the lithosphere. Hydrogen behaves as an incompatible element in NAMs and will preferentially partition into melt during melting events. As noted above, grain-boundary graphite films are unstable at temperatures greater than ~900 °C. Therefore, lithosphere that has undergone high-temperature tectonothermal and melting events is likely to have little or no remaining hydrogen or grain-boundary graphite films and will be highly resistive ($\sim 10^4$ – $10^5 \Omega\text{m}$). In contrast, lithosphere that has undergone events in which it will be enriched in incompatible elements such as interaction with fluids from a subducting slab or a plume will contain more hydrogen and carbon, leading to lower resistivities ($< \sim 10^4 \Omega\text{m}$). Electrical

resistivities of stable lithospheric regions that have been surveyed with MT show that it is not necessarily valid to assume that older lithosphere should be more resistive than younger, stable lithosphere. The most important factor to consider when interpreting MT data from stable lithosphere is whether past geological events will have resulted in a lithosphere that is enriched in incompatible elements and contains hydrogen and grain-boundary graphite films or whether past geological events will have heated and melted the lithosphere, removing hydrogen and destroying grain-boundary graphite films. Electrical conductivity measured in MT surveys can therefore be considered to be a proxy for measuring the state of enrichment in incompatible elements of the lithosphere.

Acknowledgments The manuscript benefited greatly from many conversations with those in the EM community at the 21st EMIW and the members of the TRaX and CERG research groups at the University of Adelaide. Martin Hand is thanked for his comments on the manuscript and for the countless conversations over the years which led to the ideas presented within it. Shun-Ichiro Karato provided valuable comments on the mineral physics section. The author was supported by Australian Research Council Postdoctoral Fellowship DP0988263 and National Science Foundation Grant EAR-1069423.

References

- Allegre CJ, Poirier JP, Humler E, Hofmann AW (1995) The chemical composition of the Earth. *Earth Planet Sci Lett* 134(3–4):515–526. doi:[10.1016/0012-821x\(95\)00123-t](https://doi.org/10.1016/0012-821x(95)00123-t)
- Allen SR, McPhie J, Ferris G, Simpson C (2008) Evolution and architecture of a large felsic Igneous Province in western Laurentia: the 1.6 Ga Gawler Range Volcanics, South Australia. *J Volcanol Geotherm Res* 172(1–2):132–147. doi:[10.1016/j.jvolgeores.2005.09.027](https://doi.org/10.1016/j.jvolgeores.2005.09.027)
- Artemieva IM (2006) Global 1 degrees \times 1 degrees thermal model TC1 for the continental lithosphere: implications for lithosphere secular evolution. *Tectonophysics* 416(1–4):245–277. doi:[10.1016/j.tecto.2005.11.022](https://doi.org/10.1016/j.tecto.2005.11.022)
- Artemieva IM, Mooney WD (2001) Thermal thickness and evolution of Precambrian lithosphere: a global study. *J Geophys Res Solid Earth* 106(B8):16387–16414. doi:[10.1029/2000jb900439](https://doi.org/10.1029/2000jb900439)
- Aubaud C, Hauri EH, Hirschmann MM (2004) Hydrogen partition coefficients between nominally anhydrous minerals and basaltic melts. *Geophys Res Lett* 31(20):L20611
- Aulbach S, Pearson NJ, O'Reilly SY, Doyle BJ (2007) Origins of xenolithic eclogites and pyroxenites from the central slave craton, Canada. *J Petrol* 48(10):1843–1873. doi:[10.1093/petrology/egm041](https://doi.org/10.1093/petrology/egm041)
- Banks R, Livelybrooks D, Jones P, Longstaff R (1996) Causes of high crustal conductivity beneath the Iapetus suture zone in Great Britain. *Geophys J Int* 124(2):433–455
- Becken M, Ritter O (2012) Magnetotelluric studies at the San Andreas Fault Zone: implications for the role of fluids. *Surv Geophys* 33(1):65–105. doi:[10.1007/s10712-011-9144-0](https://doi.org/10.1007/s10712-011-9144-0)
- Bell DR, Rossman GR (1992) Water in Earth's mantle—the role of nominally anhydrous minerals. *Science* 255(5050):1391–1397. doi:[10.1126/science.255.5050.1391](https://doi.org/10.1126/science.255.5050.1391)
- Bell DR, Rossman GR, Maldener J, Endisch D, Rauch F (2003) Hydroxide in olivine: a quantitative determination of the absolute amount and calibration of the IR spectrum. *J Geophys Res Solid Earth* 108(2):2105. doi:[10.1029/2001jb000679](https://doi.org/10.1029/2001jb000679)
- Bertrand E, Unsworth M, Chiang C-W, Chen C-S, Chen C-C, Wu F, Türkoğlu E, Hsu H-L, Hill G (2009) Magnetotelluric evidence for thick-skinned tectonics in central Taiwan. *Geology* 37(8):711–714
- Betts PG, Giles D, Foden J, Schaefer BF, Mark G, Pankhurst MJ, Forbes CJ, Williams HA, Chalmers NC, Hills Q (2009) Mesoproterozoic plume-modified orogenesis in eastern Precambrian Australia. *Tectonics* 28:Tc3006. doi:[10.1029/2008tc002325](https://doi.org/10.1029/2008tc002325)
- Betts PG, Giles D, Lister GS, Frick LR (2002) Evolution of the Australian lithosphere. *Aust J Earth Sci* 49(4):661–695
- Boerner D, Kurtz R, Craven J, Ross G, Jones F, Davis W (1999) Electrical conductivity in the Precambrian lithosphere of Western Canada. *Science* 283(5402):668–670
- Boerner DE, Kurtz RD, Craven JA (1996) Electrical conductivity and Paleo-Proterozoic foredeeps. *J Geophys Res Solid Earth* 101(B6):13775–13791. doi:[10.1029/96jb00171](https://doi.org/10.1029/96jb00171)
- Bologna MS, Padilha AL, Vitorello Í, Pádua MB (2011) Signatures of continental collisions and magmatic activity in central Brazil as indicated by a magnetotelluric profile across distinct tectonic provinces. *Precambrian Res* 185(1):55–64

- Booker JR, Favetto A, Pomposiello MC (2004) Low electrical resistivity associated with plunging of the Nazca flat slab beneath Argentina. *Nature* 429(6990):399–403
- Branch T, Ritter O, Weckmann U, Sachsenhofer RF, Schilling F (2007) The Whitehill Formation—a high conductivity marker horizon in the Karoo Basin. *S Afr J Geol* 110(2–3):465–476. doi:[10.2113/gssajg.110.2-3.465](https://doi.org/10.2113/gssajg.110.2-3.465)
- Brasse H, Lezaeta P, Rath V, Schwalenberg K, Soyer W, Haak V (2002) The Bolivian Altiplano conductivity anomaly. *J Geophys Res Solid Earth* 107(5):2096. doi:[10.1029/2001jb000391](https://doi.org/10.1029/2001jb000391)
- Bürgmann R, Dresen G (2008) Rheology of the lower crust and upper mantle: evidence from rock mechanics, geodesy, and field observations. *Annu Rev Earth Planet Sci* 36:531–567
- Chakraborty S (2008) Diffusion in solid silicates: a tool to track timescales of processes comes of age. In: Annual review of Earth and planetary sciences, vol 36. pp 153–190. doi:[10.1146/annurev.earth.36.031207.124125](https://doi.org/10.1146/annurev.earth.36.031207.124125)
- Chalmers N (2007) Mt Woods domain: Proterozoic metasediments and intrusives. Department of Primary Industries and Resources South Australia, Report Book 2007/20. Adelaide
- Chen CW, Rondenay S, Evans RL, Snyder DB (2009) Geophysical detection of relict metasomatism from an Archean (similar to 3.5 Ga) subduction zone. *Science* 326(5956):1089–1091. doi:[10.1126/science.1178477](https://doi.org/10.1126/science.1178477)
- Chouteau M, Zhang P, Dion DJ, Giroux B, Morin R, Krivochieva S (1997) Delineating mineralization and imaging the regional structure with magnetotellurics in the region of Chibougamau (Canada). *Geophysics* 62(3):730–748
- Christensen NI, Mooney WD (1995) Seismic velocity structure and composition of the continental-crust—a global view. *J Geophys Res Solid Earth* 100(B6):9761–9788. doi:[10.1029/95jb00259](https://doi.org/10.1029/95jb00259)
- Connolly JAD, Podladchikov YY (2004) Fluid flow in compressional tectonic settings: implications for midcrustal seismic reflectors and downward fluid migration. *J Geophys Res* 109:BO4201
- Cull JP (1982) An appraisal of Australian heat-flow data. *BMR J Aust Geol Geophys* 7(1):11–21
- Dai L, Karato S-i (2009a) Electrical conductivity of orthopyroxene: implications for the water content of the asthenosphere. *Proc Jpn Acad Ser B Phys Biol Sci* 85(10):466–475. doi:[10.2183/pjab.85.466](https://doi.org/10.2183/pjab.85.466)
- Dai L, Karato S-i (2009b) Electrical conductivity of pyrope-rich garnet at high temperature and high pressure. *Phys Earth Planet Inter* 176(1–2):83–88. doi:[10.1016/j.pepi.2009.04.002](https://doi.org/10.1016/j.pepi.2009.04.002)
- Dai L, Karato S-i (2009c) Electrical conductivity of wadsleyite at high temperatures and high pressures. *Earth Planet Sci Lett* 287(1–2):277–283. doi:[10.1016/j.epsl.2009.08.012](https://doi.org/10.1016/j.epsl.2009.08.012)
- Dai L, Li H, Hu H, Shan S, Jiang J, Hui K (2012) The effect of chemical composition and oxygen fugacity on the electrical conductivity of dry and hydrous garnet at high temperatures and pressures. *Contrib Miner Petrol* 163(4):689–700. doi:[10.1007/s00410-011-0693-5](https://doi.org/10.1007/s00410-011-0693-5)
- Daly SJ, Fanning CM, Fairclough MC (1998) Tectonic evolution and exploration potential of the Gawler Craton, South Australia. *J Aust Geol Geophys* 17(3):145–168
- Dasgupta R, Hirschmann MM (2010) The deep carbon cycle and melting in Earth's interior. *Earth Planet Sci Lett* 298(1):1–13
- Davis WJ, Jones AG, Bleeker W, Grutter H (2003) Lithosphere development in the Slave craton: a linked crustal and mantle perspective. *Lithos* 71(2–4):575–589. doi:[10.1016/s0024-4937\(03\)00131-2](https://doi.org/10.1016/s0024-4937(03)00131-2)
- Deines P (2002) The carbon isotope geochemistry of mantle xenoliths. *Earth-Sci Rev* 58(3):247–278
- Demouchy S (2010a) Diffusion of hydrogen in olivine grain boundaries and implications for the survival of water-rich zones in the Earth's mantle. *Earth Planet Sci Lett* 295(1–2):305–313. doi:[10.1016/j.epsl.2010.04.019](https://doi.org/10.1016/j.epsl.2010.04.019)
- Demouchy S (2010b) Hydrogen diffusion in spinel grain boundaries and consequences for chemical homogenization in hydrous peridotite. *Contrib Miner Petrol* 160(6):887–898. doi:[10.1007/s00410-010-0512-4](https://doi.org/10.1007/s00410-010-0512-4)
- Dixon JE, Leist L, Langmuir C, Schilling J-G (2002) Recycled dehydrated lithosphere observed in plume-influenced mid-ocean-ridge basalt. *Nature* 420(6914):385–389
- Djomani YHP, O'Reilly SY, Griffin WL, Morgan P (2001) The density structure of subcontinental lithosphere through time. *Earth Planet Sci Lett* 184(3–4):605–621
- Dmitriev VI, Berdichevsky MN (1979) The fundamental model of magnetotelluric sounding. *Proc IEEE* 67(7):1034–1044
- Du Frane WL, Roberts JJ, Toffelmier DA, Tyburczy JA (2005) Anisotropy of electrical conductivity in dry olivine. *Geophys Res Lett* 32(24):L24315
- Du Frane WL, Tyburczy JA (2012) Deuterium-hydrogen exchange in olivine: implications for point defects and electrical conductivity. *Geochem Geophys Geosyst* 13(null):Q03004
- Duba A, Heikamp S, Meurer W, Nover G, Will G (1994) Evidence from borehole samples for the role of accessory minerals in lower-crustal conductivity. *Nature* 367(6458):59–61

- Duba A, Huenges E, Nover G, Will G, Jodicke H (1988) Impedance of black shale from Munsterland-1 borehole—an anomalously good conductor. *Geophys J Oxf* 94(3):413–419
- Duba AG, Shankland TJ (1982) Free carbon and electrical-conductivity in the Earth's mantle. *Geophys Res Lett* 9(11):1271–1274
- Egbert GD, Booker JR (1992) Very long period magnetotellurics at Tuscon-observatory—implications for mantle conductivity. *J Geophys Res Solid Earth* 97(B11):15099–15112. doi:10.1029/92jb01251
- Evans RL, Jones AG, Garcia X, Muller M, Hamilton M, Evans S, Fourie C, Spratt J, Webb S, Jelsma H (2011) Electrical lithosphere beneath the Kaapvaal craton, southern Africa. *J Geophys Res* 116(B4):B04105
- Fanning CM, Reid A, Teale GS (2007) A geochronological framework for the Gawler Craton, South Australia. Geological Survey, Primary Industries and Resources South Australia. Bulletin 55
- Ferguson IJ, Craven JA, Kurtz RD, Boerner DE, Bailey RC, Wu X, Orellana MR, Spratt J, Wennberg G, Norton A (2005) Geoelectric response of Archean lithosphere in the western Superior Province, central Canada. *Phys Earth Planet Inter* 150(1–3):123–143. doi:10.1016/j.pepi.2004.08.025
- Figueiredo I, Meju M, Fontes S (2008) Heterogeneous crust and upper mantle across the SE Brazilian Highlands and the relationship to surface deformation as inferred from magnetotelluric imaging. *J Geophys Res* 113(B3):B03404
- Forbes CJ, Giles D, Jourdan F, Sato K, Omori S, Bunch M (2012) Cooling and exhumation history of the northeastern Gawler Craton, South Australia. *Precamb Res* 200:209–238. doi:10.1016/j.precamres.2011.11.003
- Fraser G, McAvaney S, Neumann N, Szpunar M, Reid A (2010) Discovery of early Mesoarchean crust in the eastern Gawler Craton, South Australia. *Precambrian Res* 179(1):1–21
- Frost BR, Fyfe WS, Tazaki K, Chan T (1989) Grain-boundary graphite in rocks and implications for high electrical-conductivity in the lower crust. *Nature* 340(6229):134–136
- Frost DJ, Mann U, Asahara Y, Rubie DC (2008) The redox state of the mantle during and just after core formation. *Philos Trans R Soc A Math Phys Eng Sci* 366(1883):4315–4337. doi:10.1098/rsta.2008.0147
- Fullea J, Muller MR, Jones AG (2011) Electrical conductivity of continental lithospheric mantle from integrated geophysical and petrological modeling: application to the Kaapvaal Craton and Rehoboth Terrane, southern Africa. *J Geophys Res Solid Earth* 116:B10202. doi:10.1029/2011jb008544
- Glover PW, Vine F (1994) Electrical conductivity of the continental crust. *Geophys Res Lett* 21(22):2357–2360
- Glover PWJ (1996) Graphite and electrical conductivity in the lower continental crust: a review. *Phys Chem Earth* 21(4):279–287
- Gokarn S, Gupta G, Rao C (2004) Geoelectric structure of the Dharwar Craton from magnetotelluric studies: Archean suture identified along the Chitradurga–Gadag schist belt. *Geophys J Int* 158(2):712–728
- Griffin WL, Doyle BJ, Ryan CG, Pearson NJ, O'Reilly SY, Davies R, Kivi K, Van Acherbergh E, Natapov LM (1999) Layered mantle lithosphere in the Lac de Gras area, Slave Craton: composition, structure and origin. *J Petrol* 40(5):705–727. doi:10.1093/petrology/40.5.705
- Griffin WL, O'Reilly SY, Afonso JC, Begg GC (2009) The composition and evolution of lithospheric mantle: a re-evaluation and its tectonic implications. *J Petrol* 50(7):1185–1204. doi:10.1093/petrology/egn033
- Griffin WL, O'Reilly SY, Doyle BJ, Pearson NJ, Coopersmith H, Kivi K, Malkovets V, Pokhilenko N (2004) Lithosphere mapping beneath the North American plate. *Lithos* 77(1–4):873–922. doi:10.1016/j.lithos.2004.03.034
- Grütter H, Apter DB, Kong J (1999) Crust-mantle coupling: Evidence from mantle-derived xenocrystic garnets. In: Gurney JJ, Gurney JL, Pascoe MD, Richardson SH (eds) Proceedings of the 7th international kimberlite conference, Cape Town, South Africa, pp 307–313
- Guo X, Yoshino T, Katayama I (2011) Electrical conductivity anisotropy of deformed talc rocks and serpentinites at 3 GPa. *Phys Earth Planet Inter* 188(1–2):69–81. doi:10.1016/j.pepi.2011.06.012
- Haak V, Hutton R (1986) Electrical resistivity in continental lower crust. *Geol Soc Lond Special Publ* 24(1):35–49
- Haggerty SE (1994) Superkimberlites—a geodynamic diamond window to the Earth's core. *Earth Planet Sci Lett* 122(1–2):57–69. doi:10.1016/0012-821x(94)90051-5
- Hand M, Reid A, Jagodzinski L (2007) Tectonic framework and evolution of the Gawler craton, southern Australia. *Econ Geol* 102(8):1377–1395
- Hand M, Sandiford M (1999) Intraplate deformation in central Australia, the link between subsidence and fault reactivation. *Tectonophysics* 305(1–3):121–140
- Hautot S, Tarits P, Whaler K, Le Gall B, Tiercelin JJ, Le Turdu C (2000) Deep structure of the Baringo Rift Basin (central Kenya) from three-dimensional magnetotelluric imaging: implications for rift evolution. *J Geophys Res Solid Earth* 105(B10):23493–23518

- Heaman LM, Pearson DG (2010) Nature and evolution of the Slave Province subcontinental lithospheric mantle. *Can J Earth Sci* 47(4):369–388. doi:[10.1139/e09-046](https://doi.org/10.1139/e09-046)
- Hedenquist JW, Lowenstern JB (1994) The role of magmas in the formation of hydrothermal ore deposits. *Nature* 370(6490):519–527. doi:[10.1038/370519a0](https://doi.org/10.1038/370519a0)
- Heinson G, Constable S (1992) The electrical- conductivity of the oceanic upper mantle. *Geophys J Int* 110(1):159–179. doi:[10.1111/j.1365-246X.1992.tb00719.x](https://doi.org/10.1111/j.1365-246X.1992.tb00719.x)
- Heinson G, Dureen NG, Gill R (2006) Magnetotelluric evidence for a deep-crustal mineralising system beneath the giant Olympic Dam iron-oxide copper gold deposit, southern Australia. *Geology* 34(7):573–576
- Hill GJ, Caldwell TG, Heise W, Chertkoff DG, Bibby HM, Burgess MK, Cull JP, Cas RAF (2009) Distribution of melt beneath Mount St Helens and Mount Adams inferred from magnetotelluric data. *Nat Geosci* 2(11):785–789. doi:[10.1038/ngeo661](https://doi.org/10.1038/ngeo661)
- Hirth G, Kohlstedt DL (1996) Water in the oceanic upper mantle: implications for rheology, melt extraction and the evolution of the lithosphere. *Earth Planet Sci Lett* 144(1–2):93–108. doi:[10.1016/0012-821x\(96\)00154-9](https://doi.org/10.1016/0012-821x(96)00154-9)
- Hjelt SE, Korja T (1993) Lithospheric and upper-mantle structures, results of electromagnetic soundings in Europe. *Phys Earth Planet Inter* 79(1–2):137–177
- Hoffmann-Rothe A, Ritter O, Haak V (2001) Magnetotelluric and geomagnetic modelling reveals zones of very high electrical conductivity in the upper crust of Central Java. *Phys Earth Planet Inter* 124(3–4):131–151
- Hofmann AW (1988) Chemical differentiation of the Earth—the relationship between mantle, continental crust and oceanic crust. *Earth Planet Sci Lett* 90(3):297–314. doi:[10.1016/0012-821x\(88\)90132-x](https://doi.org/10.1016/0012-821x(88)90132-x)
- Hofmann AW (1997) Mantle geochemistry: the message from oceanic volcanism. *Nature* 385(6613):219–229. doi:[10.1038/385219a0](https://doi.org/10.1038/385219a0)
- Hopper DJ (2001) Crustal evolution of Paleo- to Mesoproterozoic rocks in the Peake and Denison Ranges. University of Queensland, Brisbane, South Australia
- Howard KE, Hand M, Barovich KM, Payne JL, Belousova EA (2011) U-Pb, Lu-Hf and Sm-Nd isotopic constraints on provenance and depositional timing of metasedimentary rocks in the western Gawler Craton: implications for Proterozoic reconstruction models. *Precambrian Res* 184(1–4):43–62. doi:[10.1016/j.precamres.2010.10.002](https://doi.org/10.1016/j.precamres.2010.10.002)
- Howard KE, Hand M, Barovich KM, Reid A, Wade BP, Belousova EA (2009) Detrital zircon ages: improving interpretation via Nd and Hf isotopic data. *Chem Geol* 262(3–4):277–292. doi:[10.1016/j.chemgeo.2009.01.029](https://doi.org/10.1016/j.chemgeo.2009.01.029)
- Hunter RH, McKenzie D (1989) The equilibrium geometry of carbonate melts in rocks of mantle composition. *Earth Planet Sci Lett* 92(3–4):347–356. doi:[10.1016/0012-821x\(89\)90059-9](https://doi.org/10.1016/0012-821x(89)90059-9)
- Hyndman R, Hyndman D (1968) Water saturation and high electrical conductivity in the lower continental crust. *Earth Planet Sci Lett* 4(6):427–432
- Ingrin J, Skogby H (2000) Hydrogen in nominally anhydrous upper-mantle minerals: concentration levels and implications. *Eur J Mineral* 12:543–570
- Jaupart C, Mareschal J (2007) Heat flow and thermal structure of the lithosphere. *Treatise Geophys* 6:217–251
- Jödicke H, Kruhl JH, Ballhaus C, Giese P, Untiedt J (2004) Syngenetic, thin graphite-rich horizons in lower crustal rocks from the Serre San Bruno, Calabria (Italy), and implications for the nature of high-conducting deep crustal layers. *Phys Chem Earth* 141:37–58
- Jones AG (1992) Electrical conductivity of the continental lower crust. *Continental lower crust*, pp 81–143
- Jones AG (1999) Imaging the continental upper mantle using electromagnetic methods. *Lithos* 48(1–4):57–80. doi:[10.1016/s0024-4937\(99\)00022-5](https://doi.org/10.1016/s0024-4937(99)00022-5)
- Jones AG, Ferguson IJ (2001) The electric Moho. *Nature* 409(6818):331–333. doi:[10.1038/35053053](https://doi.org/10.1038/35053053)
- Jones AG, Ferguson IJ, Chave AD, Evans RL, McNeice GW (2001) Electric lithosphere of the Slave craton. *Geology* 29(5):423–426. doi:[10.1130/0091-7613\(2001\)029<0423:elotsc>2.0.co;2](https://doi.org/10.1130/0091-7613(2001)029<0423:elotsc>2.0.co;2)
- Jones AG, Fishwick S, Evans RL, Muller MR, Fullea J (2013) Velocity-conductivity relations for cratonic lithosphere and their application: example of Southern Africa. *Lithos* 109(1):131–143
- Jones AG, Ledo J, Ferguson IJ (2005a) Electromagnetic images of the Trans-Hudson Orogen: the North American Central Plains anomaly revealed. *Can J Earth Sci* 42(4):457–478
- Jones AG, Ledo J, Ferguson IJ, Farquharson C, Garcia X, Grant N, McNeice G, Roberts B, Spratt J, Wennberg G (2005b) The electrical resistivity structure of Archean to Tertiary lithosphere along 3200 km of SNORCLE profiles, northwestern Canada. *Can J Earth Sci* 42(6):1257–1275
- Jones AG, Lezaeta P, Ferguson IJ, Chave AD, Evans RL, Garcia X, Spratt J (2003) The electrical structure of the Slave craton. *Lithos* 71(2–4):505–527. doi:[10.1016/j.lithos.2003.08.001](https://doi.org/10.1016/j.lithos.2003.08.001)

- Kamenetsky VS, Crawford AJ, Meffre S (2001) Factors controlling chemistry of magmatic spinel: an empirical study of associated olivine, Cr-spinel and melt inclusions from primitive rocks. *J Petrol* 42(4):655–671. doi:[10.1093/petrology/42.4.655](https://doi.org/10.1093/petrology/42.4.655)
- Karato S-I (2011) Water distribution across the mantle transition zone and its implications for global material circulation. *Earth Planet Sci Lett* 301(3–4):413–423. doi:[10.1016/j.epsl.2010.11.038](https://doi.org/10.1016/j.epsl.2010.11.038)
- Karato S-I, Dai L (2009) Comments on “Electrical conductivity of wadsleyite as a function of temperature and water content” by Manthilake et al. *Phys Earth Planet Inter* 174(1–4):19–21. doi:[10.1016/j.pepi.2009.01.011](https://doi.org/10.1016/j.pepi.2009.01.011)
- Karato S (1990) The role of hydrogen in the electrical-conductivity of the upper mantle. *Nature* 347(6290):272–273. doi:[10.1038/347272a0](https://doi.org/10.1038/347272a0)
- Karato S (2006) Remote sensing of hydrogen in Earth’s mantle. In: Keppler HSJR (ed) *Water in nominally anhydrous minerals*, vol 62. *Reviews in mineralogy & geochemistry*, pp 343–375. doi:[10.2138/rmg.2006.62.15](https://doi.org/10.2138/rmg.2006.62.15)
- Karato S, Wu P (1993) Rheology of the upper mantle—a synthesis. *Science* 260(5109):771–778. doi:[10.1126/science.260.5109.771](https://doi.org/10.1126/science.260.5109.771)
- Katsube TJ, Mareschal M (1993) Petrophysical model of deep electrical conductors: graphite lining as a source and its disconnection due to uplift. *J Geophys Res Solid Earth* 98(B5):8019–8030
- Kelsey DE (2008) On ultrahigh-temperature crustal metamorphism. *Gondwana Res* 13(1):1–29
- Kerrick DM, Connolly JAD (1998) Subduction of ophicarbonates and recycling of CO₂ and H₂O. *Geology* 26(4):375–378. doi:[10.1130/0091-7613\(1998\)026<0375:sooar>2.3.co;2](https://doi.org/10.1130/0091-7613(1998)026<0375:sooar>2.3.co;2)
- Kerrick DM, Connolly JAD (2001a) Metamorphic devolatilization of subducted marine sediments and the transport of volatiles into the Earth’s mantle. *Nature* 411(6835):293–296. doi:[10.1038/35077056](https://doi.org/10.1038/35077056)
- Kerrick DM, Connolly JAD (2001b) Metamorphic devolatilization of subducted oceanic metabasalts: implications for seismicity, arc magmatism and volatile recycling. *Earth Planet Sci Lett* 189(1–2): 19–29. doi:[10.1016/s0012-821x\(01\)00347-8](https://doi.org/10.1016/s0012-821x(01)00347-8)
- Kohlstedt DL, Evans B, Mackwell SJ (1995) Strength of the lithosphere: constraints imposed by laboratory experiments. *J Geophys Res Solid Earth* 100(9):17587–17602. doi:[10.1029/95jb01460](https://doi.org/10.1029/95jb01460)
- Kohlstedt DL, Keppler H, Rubie DC (1996) Solubility of water in the alpha, beta and gamma phases of (Mg, Fe)₂SiO₄. *Contrib Miner Petrol* 123(4):345–357. doi:[10.1007/s004100050161](https://doi.org/10.1007/s004100050161)
- Kohlstedt DL, Mackwell SJ (1998) Diffusion of hydrogen and intrinsic point defects in olivine. *Z Phys Chem Int J Res Phys Chem Chem Phys* 207:147–162
- Korja T, Hjelt S-E (1993) Electromagnetic studies in the Fennoscandian Shield—electrical conductivity of Precambrian crust. *Phys Earth Planet Inter* 81(1):107–138
- Kovács I, Green DH, Rosenthal A, Hermann J, O’neill HSC, Hibberson WO, Udvardi B (2012) An experimental study of water in nominally anhydrous minerals in the upper mantle near the water-saturated solidus. *J Petrol* 53(10):2067–2093
- Lee C, Rudnick R (1999) Compositionally stratified cratonic lithosphere: petrology and geochemistry of peridotite xenoliths from the Labait tuff cone, Tanzania. In: *Proceedings of the 7th international Kimberlite conference*, pp 503–521
- Livelybrooks D, Mareschal M, Blais E, Smith JT (1996) Magnetotelluric delineation of the Trillabelle massive sulfide body in Sudbury, Ontario. *Geophysics* 61(4):971–986
- Lu R, Keppler H (1997) Water solubility in pyrope to 100 kbar. *Contrib Miner Petrol* 129(1):35–42. doi:[10.1007/s004100050321](https://doi.org/10.1007/s004100050321)
- Maier R, Heinson G, Thiel S, Selway K, Gill R, Scroggs M (2007) A 3D lithospheric electrical resistivity model of the Gawler Craton, Southern Australia. *Appl Earth Sci* 116:13–21
- Mareschal M, Fyfe WS, Percival J, Chan T (1992) Grain-boundary graphite in Kapuskasing gneisses and implications for lower-crustal conductivity. *Nature* 357(6380):674–676
- Mareschal M, Kellellt RL, Kurtz RD, Ludden JN, Ji S, Bailey RC (1995) Archean cratonic roots, mantle shear zones and deep electrical anisotropy. *Nature* 375(6527):134–137. doi:[10.1038/375134a0](https://doi.org/10.1038/375134a0)
- Marty B, Tolstikhin IN (1998) CO₂ fluxes from mid-ocean ridges, arcs and plumes. *Chem Geol* 145(3–4):233–248. doi:[10.1016/s0009-2541\(97\)00145-9](https://doi.org/10.1016/s0009-2541(97)00145-9)
- Mathez EA (1987) Carbonaceous matter in mantle xenoliths—composition and relevance to the isotopes. *Geochim Cosmochim Acta* 51(9):2339–2347. doi:[10.1016/0016-7037\(87\)90288-2](https://doi.org/10.1016/0016-7037(87)90288-2)
- Mathez EA, Dietrich VJ, Irving AJ (1984) The geochemistry of carbon in mantle peridotites. *Geochim Cosmochim Acta* 48(9):1849–1859. doi:[10.1016/0016-7037\(84\)90038-3](https://doi.org/10.1016/0016-7037(84)90038-3)
- Mathez EA, Duba AG, Peach CL, Leger A, Shankland TJ, Plafker G (1995) Electrical-conductivity and carbon in metamorphic rocks of the Yukon-Tanana Terrane, Alaska. *J Geophys Res Solid Earth* 100(B6):10187–10196
- McDonough WF, Sun SS (1995) The composition of the Earth. *Chem Geol* 120(3–4):223–253. doi:[10.1016/0009-2541\(94\)00140-4](https://doi.org/10.1016/0009-2541(94)00140-4)

- McFarlane CRM (2006) Palaeoproterozoic evolution of the Challenger Au deposit, South Australia, from monazite geochronology. *J Metamorph Geol* 24(1):75–87. doi:[10.1111/j.1525-1314.2005.00622.x](https://doi.org/10.1111/j.1525-1314.2005.00622.x)
- McKenzie D, Jackson J, Priestley K (2005) Thermal structure of oceanic and continental lithosphere. *Earth Planet Sci Lett* 233(3–4):337–349. doi:[10.1016/j.epsl.2005.02.005](https://doi.org/10.1016/j.epsl.2005.02.005)
- McLaren S, Sandiford M, Powell R (2005) Contrasting styles of proterozoic crustal evolution: a hot-plate tectonic model for Australian terranes. *Geology* 33(8):673–676. doi:[10.1130/g21544](https://doi.org/10.1130/g21544)
- Meqbel NM, Ritter O (2013) A magnetotelluric transect across the Dead Sea Basin: electrical properties of geological and hydrological units of the upper crust. *Geophys J Int.* doi: [10.1093/gji/ggt051](https://doi.org/10.1093/gji/ggt051)
- Michael PJ (1988) The concentration, behaviour and storage of H₂O in the suboceanic upper mantle—implications for mantle metasomatism. *Geochim Cosmochim Acta* 52(2):555–566. doi:[10.1016/0016-7037\(88\)90110-x](https://doi.org/10.1016/0016-7037(88)90110-x)
- Michaut C, Jaupart C, Mareschal JC (2009) Thermal evolution of cratonic roots. *Lithos* 109(1):47–60
- Mierdel K, Keppler H, Smyth JR, Langenhorst F (2007) Water solubility in aluminous orthopyroxene and the origin of Earth's asthenosphere. *Science* 315(5810):364–368. doi:[10.1126/science.1135422](https://doi.org/10.1126/science.1135422)
- Mookherjee M, Karato S-i (2010) Solubility of water in pyrope-rich garnet at high pressures and temperature. *Geophys Res Lett* 37:L03310. doi:[10.1029/2009gl014289](https://doi.org/10.1029/2009gl014289)
- Moore JC, Vrolijk P (1992) Fluids in accretionary prisms. *Rev Geophys* 30(2):113–135. doi: [10.1029/92rg00201](https://doi.org/10.1029/92rg00201)
- Morrissey L, Payne JL, Kelsey DE, Hand M (2011) Grenvilli an-aged reworking in the North Australian Craton, central Australia: constraints from geochronology and modelled phase equilibria. *Precambrian Res* 191(3–4):141–165. doi:[10.1016/j.precamres.2011.09.010](https://doi.org/10.1016/j.precamres.2011.09.010)
- Muller M, Jones A, Evans R, Grütter H, Hatton C, Garcia X, Hamilton M, Miensoop M, Cole P, Ngwisanyi T (2009) Lithospheric structure, evolution and diamond prospectivity of the Rehoboth Terrane and western Kaapvaal Craton, southern Africa: constraints from broadband magnetotellurics. *Lithos* 112:93–105
- Naganjaneyulu K, Santosh M (2012) The nature and thickness of lithosphere beneath the Archean Dharwar Craton, southern India: a magnetotelluric model. *J Asian Earth Sci* 49:349–361
- Neumann N, Sandiford M, Foden J (2000) Regional geochemistry and continental heat flow: implications for the origin of the South Australian heat flow anomaly. *Earth Planet Sci Lett* 183(1–2):107–120. doi: [10.1016/S0012-821X\(00\)00268-5](https://doi.org/10.1016/S0012-821X(00)00268-5)
- Nyblade AA, Pollack HN (1993) A global analysis of heat-flow from Precambrian terrains—implications for the thermal structure of Archean and Proterozoic lithosphere. *J Geophys Res Solid Earth* 98(B7): 12207–12218. doi:[10.1029/93jb00521](https://doi.org/10.1029/93jb00521)
- Nyblade AA, Pollack HN, Jones DL, Podmore F, Mushayandebvu M (1990) Terrestrial heat-flow in east and southern Africa. *J Geophys Res Solid Earth Planets* 95(B11):17371–17384. doi:[10.1029/JB095iB11p1737](https://doi.org/10.1029/JB095iB11p1737)
- Ogawa Y, Jones AG, Unsworth MJ, Booker JR, Lu X, Craven J, Roberts B, Parmelee J, Farquharson C (1996) Deep electrical conductivity structures of the Appalachian Orogen in the southeastern US. *Geophys Res Lett* 23(13):1597–1600
- Ohmoto H (1986) Stable isotope geochemistry of ore deposits. *Rev Miner* 16:491–559
- Patro PK, Sarma S (2009) Lithospheric electrical imaging of the Deccan trap covered region of western India. *J Geophys Res* 114(B1):B01102
- Payne JL, Barovich K, Hand M (2006) Provenance of metasedimentary rocks in the northern Gawler Craton, Australia: implications for Palaeoproterozoic reconstructions. *Precambrian Res* 148(3–4):275–291
- Payne JL, Hand M, Barovich KM, Reid A, Evans DAD (2009) Correlations and reconstruction models for the 2500–1500 Ma evolution of the Mawson Continent. In: Reddy SM, Mazumder R, Evans DAD, Collins AS (eds) *Palaeoproterozoic supercontinents and global evolution*, vol 323. Geological Society, London, Special Publications, pp 319–356
- Payne JL, Hand M, Barovich KM, Wade BP (2008) Temporal constraints on the timing of high-grade metamorphism in the northern Gawler Craton: implications for assembly of the Australian Proterozoic. *Aust J Earth Sci* 55(5):623–640. doi:[10.1080/08120090801982595](https://doi.org/10.1080/08120090801982595)
- Pearson D, Boyd F, Haggerty S, Pasteris J, Field S, Nixon P, Pokhilenko N (1994) The characterisation and origin of graphite in cratonic lithospheric mantle: a petrological carbon isotope and Raman spectroscopic study. *Contrib Miner Petrol* 115(4):449–466
- Pearson NJ, Griffin WL, Doyle BJ, O'Reilly SY, Van Acherbergh E, Kivi K (1999) Xenoliths from kimberlite pipes of the Lac de Gras area, Slave Craton, Canada. In: Gurney JJ, Gurney JL, Pascoe MD, Richardson SH (eds) *Proceedings of the 7th international Kimberlite conference*, vol 2. Red Roof Design, Cape Town, South Africa, pp 644–658

- Pineau F, Mathez EA (1990) Carbon isotopes in xenoliths from the Hualalai volcano, Hawaii, and the generation of isotopic variability. *Geochimica Et Cosmochimica Acta* 54(1):217–227. doi:[10.1016/0016-7037\(90\)90209-4](https://doi.org/10.1016/0016-7037(90)90209-4)
- Plank T, Langmuir CH (1998) The chemical composition of subducting sediment and its consequences for the crust and mantle. *Chem Geol* 145(3–4):325–394. doi:[10.1016/s0009-2541\(97\)00150-2](https://doi.org/10.1016/s0009-2541(97)00150-2)
- Poe BT, Romano C, Nestola F, Smyth JR (2010) Electrical conductivity anisotropy of dry and hydrous olivine at 8 GPa. *Phys Earth Planet Inter* 181(3–4):103–111. doi:[10.1016/j.pepi.2010.05.003](https://doi.org/10.1016/j.pepi.2010.05.003)
- Pommier A (2013) Interpretation of magnetotelluric results using laboratory measurements. *Surv Geophys*. doi:[10.1007/s10712-013-9226-2](https://doi.org/10.1007/s10712-013-9226-2)
- Pous J, Munoz G, Heise W, Melgarejo JC, Quesada C (2004) Electromagnetic imaging of Variscan crustal structures in SW Iberia: the role of interconnected graphite. *Earth Planet Sci Lett* 217:435–450
- Reynard B, Mibe K, van de Moortele B (2011) Electrical conductivity of the serpentinised mantle and fluid flow in subduction zones. *Earth Planet Sci Lett* 307(3–4):387–394. doi:[10.1016/j.epsl.2011.05.013](https://doi.org/10.1016/j.epsl.2011.05.013)
- Ritter O, Hoffmann-Rothe A, Bedrosian PA, Weckmann U, Haak V (2005) Electrical conductivity images of active and fossil fault zones. *High Strain Zones Struct Phys Prop* 245:165–186. doi:[10.1144/gsl.sp.2005.245.01.08](https://doi.org/10.1144/gsl.sp.2005.245.01.08)
- Rudnick RL, Fountain DM (1995) Nature and composition of the continental-crust—a lower crustal perspective. *Rev Geophys* 33(3):267–309. doi:[10.1029/95rg01302](https://doi.org/10.1029/95rg01302)
- Rudnick RL, McDonough WF, O'Connell RJ (1998) Thermal structure, thickness and composition of continental lithosphere. *Chem Geol* 145(3–4):395–411. doi:[10.1016/s0009-2541\(97\)00151-4](https://doi.org/10.1016/s0009-2541(97)00151-4)
- Sack RO, Ebel DS (2006) Thermochemistry of sulfide mineral solutions. In: Vaughan DJ (ed) *Sulfide mineralogy and geochemistry*, vol 61. *Reviews in mineralogy & geochemistry*, pp 265–364. doi:[10.2138/rmg.2006.61.6](https://doi.org/10.2138/rmg.2006.61.6)
- Sano Y, Marty B (1995) Origin of carbon in fumarolic gas from island arcs. *Chem Geol* 119(1):265–274
- Santos FAM, Mateus A, Almeida EP, Pous J, Mendes-Victor LA (2002) Are some of the deep crustal conductive features found in SW Iberia caused by graphite? *Earth Planet Sci Lett* 201(2):353–367
- Schilling FR, Partzsch GM, Brasse H, Schwarz G (1997) Partial melting below the magmatic arc in the central Andes deduced from geoelectromagnetic field experiments and laboratory data. *Phys Earth Planet Inter* 103(1–2):17–31. doi:[10.1016/s0031-9201\(97\)00011-3](https://doi.org/10.1016/s0031-9201(97)00011-3)
- Schock RN, Duba AG, Shankland TJ (1989) Electrical conduction in olivine. *J Geophys Res Solid Earth Planets* 94(B5):5829–5839. doi:[10.1029/JB094iB05p05829](https://doi.org/10.1029/JB094iB05p05829)
- Scrimgeour I, Close D (1999) Regional high-pressure metamorphism during intracratonic deformation: the Petermann Orogeny, central Australia. *J Metamorph Geol* 17(5):557–572
- Selway K, Hand M, Heinson GS, Payne JL (2009a) Magnetotelluric constraints on subduction polarity: reversing reconstruction models for Proterozoic Australia. *Geology* 37(9):799–802. doi:[10.1130/g30175a.1](https://doi.org/10.1130/g30175a.1)
- Selway K, Sheppard S, Thorne AM, Johnson SP, Groenewald PB (2009b) Identifying the lithospheric structure of a Precambrian orogen using magnetotellurics: the Capricorn Orogen, Western Australia. *Precambrian Res* 168(3–4):185–196. doi:[10.1016/j.precamres.2008.09.010](https://doi.org/10.1016/j.precamres.2008.09.010)
- Selway K, Thiel S, Key K (2012) A simple 2-D explanation for negative phases in TE magnetotelluric data. *Geophys J Int* 188(3):945–958. doi:[10.1111/j.1365-246X.2011.05312.x](https://doi.org/10.1111/j.1365-246X.2011.05312.x)
- Selway KM, Hand M, Payne JL, Heinson GS, Reid A (2011) Magnetotelluric constraints on the tectonic setting of Grenville-aged orogenesis in central Australia. *J Geol Soc* 168(1):251–264. doi:[10.1144/0016-76492010-034](https://doi.org/10.1144/0016-76492010-034)
- Sleep NH (2009) Stagnant lid convection and carbonate metasomatism of the deep continental lithosphere. *Geochem Geophys Geosyst* 10:Q11010
- Stagno V, Frost DJ (2010) Carbon speciation in the asthenosphere: experimental measurements of the redox conditions at which carbonate-bearing melts coexist with graphite or diamond in peridotite assemblages. *Earth Planet Sci Lett* 300(1):72–84
- Stern RJ (2002) Subduction zones. *Rev Geophys* 40(4):1012. doi:[10.1029/2001rg000108](https://doi.org/10.1029/2001rg000108)
- Stewart KP, Foden J (2003) Mesoproterozoic granites of South Australia. South Australia Department of Primary Industries and Resources, Report Book, vol 2003/15
- Swain G, Barovich K, Hand M, Ferris G, Schwarz M (2008) Petrogenesis of the St Peter Suite, southern Australia: arc magmatism and Proterozoic crustal growth of the South Australian Craton. *Precambrian Res* 166(1–4):283–296. doi:[10.1016/j.precamres.2007.07.028](https://doi.org/10.1016/j.precamres.2007.07.028)
- Swain G, Woodhouse A, Hand M, Barovich K, Schwarz M, Fanning CM (2005) Provenance and tectonic development of the late Archaean Gawler Craton, Australia; U-Pb zircon, geochemical and Sm-Nd isotopic implications. *Precambrian Res* 141(3–4):106–136
- Tappert R, Stachel T, Harris JW, Muehlenbachs K, Ludwig T, Brey GP (2005) Subducting oceanic crust: the source of deep diamonds. *Geology* 33(7):565–568

- Taylor SR, McLennan SM (1995) The geochemical evolution of the continental crust. *Rev Geophys* 33(2):241–265. doi:[10.1029/95rg00262](https://doi.org/10.1029/95rg00262)
- ten Grotenhuis SM, Drury MR, Peach CJ, Spiers CJ (2004) Electrical properties of fine-grained olivine: evidence for grain boundary transport. *J Geophys Res Solid Earth* 109(B6):B06203. doi:[10.1029/2003jb002799](https://doi.org/10.1029/2003jb002799)
- ten Grotenhuis SM, Drury MR, Spiers CJ, Peach CJ (2005) Melt distribution in olivine rocks based on electrical conductivity measurements. *J Geophys Res Solid Earth* 110(B12):1978–2012
- Thiel S, Heinson G (2010) Crustal imaging of a mobile belt using magnetotellurics: an example of the Fowler Domain in South Australia. *J Geophys Res Solid Earth* 115:B06102. doi:[10.1029/2009jb006698](https://doi.org/10.1029/2009jb006698)
- Tomkins AG, Mavrogenes JA (2002) Mobilization of gold as a polymetallic melt during pelite anatexis at the Challenger deposit, South Australia: a metamorphosed Archean gold deposit. *Econ Geol Bull Soc Econ Geol* 97(6):1249–1271
- Tournerie B, Chouteau M (2005) Three-dimensional magnetotelluric survey to image structure and stratigraphy of a sedimentary basin in Hungary. *Phys Earth Planet Inter* 150(1–3):197–212
- Ulmer P, Trommsdorff V (1995) Serpentine stability to mantle depths and subduction-related magmatism. *Science* 268(5212):858–861. doi:[10.1126/science.268.5212.858](https://doi.org/10.1126/science.268.5212.858)
- van Achterbergh E, Griffin WL, Ryan CG, O'Reilly SY, Pearson NJ, Kivi K, Doyle BJ (2002) Subduction signature for quenched carbonatites from the deep lithosphere. *Geology* 30(8):743–746. doi:[10.1130/0091-7613\(2002\)030<0743:ssfqcf>2.0.co;2](https://doi.org/10.1130/0091-7613(2002)030<0743:ssfqcf>2.0.co;2)
- van Achterbergh E, Griffin WL, Ryan CG, O'Reilly SY, Pearson NJ, Kivi K, Doyle BJ (2004) Melt inclusions from the deep Slave lithosphere: implications for the origin and evolution of mantle-derived carbonatite and kimberlite. *Lithos* 76(1–4):461–474. doi:[10.1016/j.lithos.2004.04.007](https://doi.org/10.1016/j.lithos.2004.04.007)
- Wade BP, Barovich KM, Hand M, Scrimgeour IR, Close DF (2006) Evidence for early Mesoproterozoic arc magmatism in the Musgrave Block, central Australia: implications for Proterozoic crustal growth and tectonic reconstructions of Australia. *J Geol* 114(1):43–63
- Wade BP, Kelsey DE, Hand M, Barovich KM (2008) The Musgrave Province: stitching north, west and south Australia. *Precambrian Res* 166(1–4):370–386. doi:[10.1016/j.precamres.2007.05.007](https://doi.org/10.1016/j.precamres.2007.05.007)
- Wang D, Karato S-I, Liu Z (2012) Influence of hydrogen on the electronic states of olivine: implications for electrical conductivity. *Geophys Res Lett* 39:L06306. doi:[10.1029/2012gl0151046](https://doi.org/10.1029/2012gl0151046)
- Wang D, Mookherjee M, Xu Y, Karato S-i (2006) The effect of water on the electrical conductivity of olivine. *Nature* 443(7114):977–980. doi:[10.1038/nature05256](https://doi.org/10.1038/nature05256)
- Wannamaker PE (2000) Comment on ‘‘The petrologic case for a dry lower crust’’ by Bruce WD Yardley and John W. Valley. *J Geophys Res* 105:6057–6064
- Wannamaker PE (2005) Anisotropy versus heterogeneity in continental solid earth electromagnetic studies: fundamental response characteristics and implications for physicochemical state. *Surv Geophys* 26(6):733–765. doi:[10.1007/s10712-005-1832-1](https://doi.org/10.1007/s10712-005-1832-1)
- Wannamaker PE, Caldwell TG, Jiracek GR, Maris V, Hill GJ, Ogawa Y, Bibby HM, Bennie SL, Heise W (2009) Fluid and deformation regime of an advancing subduction system at Marlborough, New Zealand. *Nature* 460(7256):733–736. doi:[10.1038/nature08204](https://doi.org/10.1038/nature08204)
- Wannamaker PE, Jiracek GR, Stodt JA, Caldwell TG, Gonzalez VM, McKnight JD, Porter AD (2002) Fluid generation and pathways beneath an active compressional orogen, the New Zealand Southern Alps, inferred from magnetotelluric data. *J Geophys Res Solid Earth* 107(B6):2117. doi:[10.1029/2001bj000186](https://doi.org/10.1029/2001bj000186)
- Watson HC, Roberts JJ, Tyburczy JA (2010) Effect of conductive impurities on electrical conductivity in polycrystalline olivine. *Geophys Res Lett* 37(2):L02302
- Wingate MTD, Pirajno F, Morris PA (2004) Warakurna large igneous province: a new Mesoproterozoic large igneous province in west-central Australia. *Geology* 32(2):105–108. doi:[10.1130/g20171.1](https://doi.org/10.1130/g20171.1)
- Wood BJ, Bryndzia LT, Johnson KE (1990) Mantle oxidation state and its relationship to tectonic environment and fluid speciation. *Science* 248(4953):337–345. doi:[10.1126/science.248.4953.337](https://doi.org/10.1126/science.248.4953.337)
- Workman RK, Hart SR (2005) Major and trace element composition of the depleted MORB mantle (DMM). *Earth Planet Sci Lett* 231(1–2):53–72. doi:[10.1016/j.epsl.2004.12.005](https://doi.org/10.1016/j.epsl.2004.12.005)
- Workman RK, Hauri E, Hart SR, Wang J, Blusztajn J (2006) Volatile and trace elements in basaltic glasses from Samoa: implications for water distribution in the mantle. *Earth Planet Sci Lett* 241(3):932–951
- Wyllie PJ (1980) The origin of kimberlite. *J Geophys Res* 85(NB12):6902–6910. doi:[10.1029/JB085iB12p06902](https://doi.org/10.1029/JB085iB12p06902)
- Xu YS, Shankland TJ (1999) Electrical conductivity of orthopyroxene and its high pressure phases. *Geophys Res Lett* 26(17):2645–2648. doi:[10.1029/1999gl008378](https://doi.org/10.1029/1999gl008378)
- Xu YS, Shankland TJ, Duba AG (2000) Pressure effect on electrical conductivity of mantle olivine. *Phys Earth Planet Inter* 118(1–2):149–161. doi:[10.1016/s0031-9201\(99\)00135-1](https://doi.org/10.1016/s0031-9201(99)00135-1)

- Yang X (2011) Origin of high electrical conductivity in the lower continental crust: a review. *Surv Geophys* 32(6):875–903
- Yang X, Heidelbach F (2012) Grain size effect on the electrical conductivity of clinopyroxene. *Contrib Mineral Petrol* 163(6):939–947
- Yang X, Keppler H, McCammon C, Ni H (2012) Electrical conductivity of orthopyroxene and plagioclase in the lower crust. *Contrib Miner Petrol* 163(1):33–48. doi:[10.1007/s00410-011-0657-9](https://doi.org/10.1007/s00410-011-0657-9)
- Yang X, Keppler H, McCammon C, Ni H, Xia Q, Fan Q (2011) Effect of water on the electrical conductivity of lower crustal clinopyroxene. *J Geophys Res Solid Earth* 116:B04208. doi:[10.1029/2010jb008010](https://doi.org/10.1029/2010jb008010)
- Yardley B, Valley J (1997) The petrologic case for a dry lower crust. *J Geophys Res* 102:173–185
- Yoshino T (2010) Laboratory electrical conductivity measurement of mantle minerals. *Surv Geophys* 31(2):163–206. doi:[10.1007/s10712-009-9084-0](https://doi.org/10.1007/s10712-009-9084-0)
- Yoshino T, Matsuzaki T, Shatskiy A, Katsura T (2009) The effect of water on the electrical conductivity of olivine aggregates and its implications for the electrical structure of the upper mantle. *Earth Planet Sci Lett* 288(1–2):291–300. doi:[10.1016/j.epsl.2009.09.032](https://doi.org/10.1016/j.epsl.2009.09.032)
- Yoshino T, Matsuzaki T, Yamashita S, Katsura T (2006) Hydrous olivine unable to account for conductivity anomaly at the top of the asthenosphere. *Nature* 443(7114):973–976. doi:[10.1038/nature05223](https://doi.org/10.1038/nature05223)
- Yoshino T, Nishi M, Matsuzaki T, Yamazaki D, Katsura T (2008) Electrical conductivity of majorite garnet and its implications for electrical structure in the mantle transition zone. *Phys Earth Planet Inter* 170(3–4):193–200. doi:[10.1016/j.pepi.2008.04.009](https://doi.org/10.1016/j.pepi.2008.04.009)
- Yoshino T, Noritake F (2011) Unstable graphite films on grain boundaries in crustal rocks. *Earth Planet Sci Lett* 306(3–4):186–192. doi:[10.1016/j.epsl.2011.04.003](https://doi.org/10.1016/j.epsl.2011.04.003)
- Yoshino T, Shimojuku A, Shan S, Guo X, Yamazaki D, Ito E, Higo Y, Funakoshi K-i (2012) Effect of temperature, pressure and iron content on the electrical conductivity of olivine and its high-pressure polymorphs. *J Geophys Res* 117(B8):B08205
- Zhao D (2001) Seismic structure and origin of hotspots and mantle plumes. *Earth Planet Sci Lett* 192(3):251–265. doi:[10.1016/s0012-821x\(01\)00465-4](https://doi.org/10.1016/s0012-821x(01)00465-4)
- Zhao JX, McCulloch MT, Korsch RJ (1994) Characterization of a plume-related similar to 800 Ma magmatic event and its implications for basin formation in central-southern Australia. *Earth Planet Sci Lett* 121(3–4):349–367